MOUNTAIN-PLAINS CONSORTIUM

MPC 21-437 | A. Kode, J. van de Lindt, and M.O. Amini

Investigation of Cross Timber Bridge Decks as a Sustainable Solution for Repair of Deficient Rural Wood Bridges

MOUNTAIN-PLAINS CONSORTIUM REGION 8

A University Transportation Center sponsored by the U.S. Department of Transportation serving the Mountain-Plains Region. Consortium members:

Colorado State University
North Dakota State University
South Dakota State University
University of Colorado Denver
University of Denver
University of Utah
Utah State University
University of Wyoming

Investigation of Cross Timber Bridge Decks as a Sustainable Solution for Repair of Deficient Rural Wood Bridges

Anirudh Kode
John W. van de Lindt
M. Omar Amini

Colorado State University
Fort Collins, Colorado

May 2021

Acknowledgements

We would like to extend our special gratitude to Mr. Philip Line, Director of Structural Engineering with the American Wood Council for his never-ending support and guidance in this project. His time and help were instrumental in the finishing of this project. Special thanks to Kelly Cobeen and Daniel Dolan.

We would like to extend our gratitude to Mountain-Plains Consortium for partial funding of the tests, without which this project would not have been possible.

Disclaimer

EXECUTIVE SUMMARY

Cross Laminated Timber (CLT) has only recently garnered attention as a new construction material in the United States. Despite being introduced in Europe nearly 20 years ago, CLT is still not used widely in North America. One primarily reason is because CLT is not yet recognized as a structural system for seismically active regions of the country. One sub-assembly that has not been fully investigated are horizontal diaphragms for floors, roofs, or bridge decks. This report aims to test a single large-scale CLT cantilever diaphragm subjected to a simulated seismic load. Data were collected and the behavior of the diaphragm documented to help begin to reduce this dearth of CLT data in the United States. These data will also assist in refining CLT diaphragm design procedures that have recently been developed.

Ten CLT panels were used to build the diaphragm, which was set up as a cantilever beam according to ASTM specifications. A 110-kip actuator was used to apply a concentrated load at one end of the diaphragm while a steel base serving as a fixed boundary condition was at the other end. The CUREE test protocol with a reference displacement of 75.6 mm (3 inches) was applied to the floor diaphragm specimen, which included a number of string potentiometers to collect displacement data. The diaphragm behaved in a predictable manner and the connectors initially failed in tension first even with a chord designed per the National Design Specification (NDS) for wood. Then the CLT panels separated, resulting in a total failure. This dataset will be made available to those working on CLT diaphragm provisions for refinement of ongoing revisions.

TABLE OF CONTENTS

LIST OF TABLES

LIST OF FIGURES

LIST OF ABBREVIATIONS AND SYMBOLS

A	Area of Cross Section
A_{chord}	Area of chord member
$A_{PARALLEL}$	Area of Layers with Fibers Running Parallel to the Direction of the Load
A_{NET}	Net Area
A_{eff}	Effective cross-sectional area
C_D	Load Duration Factor
C_{di}	Diaphragm Factor
C_M	Wet Service Factor
Ct	Temperature Factor
Cg	Group Action Factor
Ceg	End Grain Factor
Ctn	Toe-Nail factor
D	Major Diameter
d	Minor Diameter
D_r	Root Diameter
DL	Dead Load
E	Modulus of Elasticity
$EI_{eff,0}$	Stiffness for Beam Stability and Column Stability Calculations
EI_{app}	Apparent Bending Stiffness of CLT Including Shear Deflection
$EI_{app\text{-}min}$	Apparent Bending Stiffness of CLT for Panel Buckling Stability Calculations
F_b	Bending Design Value
F_t	Tension Design Value
$F_{c\perp}$	Compression Design Value Perpendicular to Grain
$F_{cPARALLEL}$	Compression Design Value Parallel to Grain
F_{yb}	Bending Yield Strength
$F_{C,0}$	Allowable Compression Strength

F_{T0}	Allowable Tensile Strength
G	Specific Gravity
$GA_{eff,0}$	Shear Stiffness
I	Moment of Inertia
K	Stiffness Coefficient
L	Length
L_e	Effective Length
M	Moment
M_{ALLOW}	Allowable Moment
M_{DL}	Moment due to Dead Load
P	Total Concentrated Load
P_{ALLOW}	Allowable Load Capacity
t	Thickness
t_s	Steel Thickness
V_{EQ}	Shear Load
W	Width
W_{EQ}	Seismic Load
Z	Reference Design Value
Z’	Adjusted Design Value

1. INTRODUCTION

1.1 Background and Brief History of CLT

Cross-laminated timber (CLT) was introduced in Europe in the 1990s. It is a new kind of wood product. After a good amount of research done on CLT in Europe, it is now being used for small single-family residential buildings as well as larger buildings (residential and non-residential). CLT is not as common in North America. However, Canada and the United States have recently started research on CLT, which is known to have some advantages over conventional construction materials like steel and concrete. CLT is eco-friendly and lightweight compared with these other materials. CLT research has shown us that it can offer good thermal and sound insulation, making it a very cost-competitive solution for certain applications. This has resulted in the rising popularity of CLT in the last two decades (CLT Handbook, U.S. Edition, FPInnovations, 2013).

Since 2015, various research institutions in Europe conducted research on CLT. Some notable examples include Graz University of Technology in Austria (Schickhofer et al., 2016), ETH in Switzerland (Fink et al. 2015), and TUM in Germany (Brandner & Dietsch et al., 2015). A survey was conducted to gather knowledge about CLT. According to the survey, the level of awareness of CLT in the European construction industry is low (Espinoza et al., 2016). CLT adoption as a construction material has some barriers such as building code compatibility, technical information availability, cost of wood, and misconceptions about wood and the amount of wood required for construction. Structural performance and connections were considered the most important research need (Espinoza et al., 2016).

Canada began investigating CLT to provide alternative wood products to the construction industry. Canada published the Canadian edition of the CLT Handbook (FPInnovations, 2011). This has resulted in progress in the study and use of CLT. The U.S. CLT Handbook was published shortly after in 2013. Since then, this book has helped serve as a guideline for U.S. CLT projects (FPInnovations, 2013).

The PRG 320 standard (ANSI/APA PRG 320-2012) was published in 2012. This standard specifies different grades of CLT and testing methods to ensure standard performance of the wood material itself under certain loading (and other) conditions. CLT manufacturers have for the most part accepted this standard for grading. The American Wood Council helped add a new CLT Chapter to the National Design Specification (NDS) 2015 edition (NDS, 2012). Chapters 12 and 16 of the NDS also include special provisions for CLT. Similar efforts were made in Canada. The Canadian National Standard for Engineering Design in Wood (CSA086) referenced PRG 320. CSA086 was referenced in the National Building Code of Canada (NBCC) and the International Building Code (IBC-2015) referenced the NDS-2015 edition. So CLT can be used in major constructions (Pei et al., 2016).

The PRG 320 standard has a set of CLT grades depending on the strength of the lumber boards used in the layup process to make the product. Table 1.1 gives detailed information about different grades of CLT and the type of lumber used to make them. Figures 1.1 and 1.2 include physical properties of CLT grades and further details about them. Other CLT grades are not listed in the Table 1.1, but they are permitted under certain provisions (ANSI APA PRG 320).

Table 1.1 Different Grades of CLT (ANSI APA PRG 320)

CLT Grade	Parallel Layers	Perpendicular Layers
E1	1950f – 1.7E MSR SPF	#3 Spruce Pine Fir
E2	1650f – 1.5E MSR DFL	#3 Douglas Fir Larch
E3	1200f – 1.2E MSR Misc.	#3 Misc.
E4	1950f – 1.7E MSR SP	#3 Southern Pine
V1	#2 Douglas Fir Larch	#3 Douglas Fir Larch
V2	#1/#2 Spruce Pine Fir	#3 Spruce Pine Fir
V3	#2 Southern Pine	#3 Southern Pine

Figure 1.1 shows different grades of CLT and allowable design properties in the minor and major strength directions.

	Major Strength Direction						Minor Strength Direction					
CLT Grades	$F_{b,0}$ (psi)	E_0 (10^6 psi)	$F_{t,0}$ (psi)	$F_{c,0}$ (psi)	$F_{v,0}$ (psi)	$F_{s,0}$ (psi)	$F_{b,90}$ (psi)	E_{90} (10^6 psi)	$F_{t,90}$ (psi)	$F_{c,90}$ (psi)	$F_{v,90}$ (psi)	$F_{s,90}$ (psi)
E1	1,950	1.7	1,375	1,800	135	45	500	1.2	250	650	135	45
E2	1,650	1.5	1,020	1,700	180	60	525	1.4	325	775	180	60
E3	1,200	1.2	600	1,400	110	35	350	0.9	150	475	110	35
E4	1,950	1.7	1,375	1,800	175	55	575	1.4	325	825	175	55
V1	900	1.6	575	1,350	180	60	525	1.4	325	775	180	60
V2	875	1.4	450	1,150	135	45	500	1.2	250	650	135	45
V3	975	1.6	550	1,450	175	55	575	1.4	325	825	175	55

Figure 1.1 CLT Grades and Design Properties (ANSI APA PRG 320)

Figure 1.2 illustrates lamination thicknesses in different layers of CLT panels of different sizes and grades. Also included are bending strength values in major and minor strength directions.

CLT Grade	CLT t (in.)	Lamination Thickness (in.) in CLT Layup							Major Strength Direction			Minor Strength Direction		
		=	⊥	=	⊥	=	⊥	=	$F_bS_{eff,0}$ (lbf-ft/ft)	$EI_{eff,0}$ (10^6 lbf-in.^{2}/ft)	$GA_{eff,0}$ (10^6 lbf/ft)	$F_bS_{eff,90}$ (lbf-ft/ft)	$EI_{eff,90}$ (10^6 lbf-in.^{2}/ft)	$GA_{eff,90}$ (10^6 lbf/ft)
E1	4 1/8	1 3/8	1 3/8	1 3/8					4,525	115	0.46	160	3.1	0.61
	6 7/8	1 3/8	1 3/8	1 3/8	1 3/8	1 3/8			10,400	440	0.92	1,370	81	1.2
	9 5/8	1 3/8	1 3/8	1 3/8	1 3/8	1 3/8	1 3/8	1 3/8	18,375	1,089	1.4	3,125	309	1.8
E2	4 1/8	1 3/8	1 3/8	1 3/8					3,825	102	0.53	165	3.6	0.56
	6 7/8	1 3/8	1 3/8	1 3/8	1 3/8	1 3/8			8,825	389	1.1	1,430	95	1.1
	9 5/8	1 3/8	1 3/8	1 3/8	1 3/8	1 3/8	1 3/8	1 3/8	15,600	963	1.6	3,275	360	1.7
E3	4 1/8	1 3/8	1 3/8	1 3/8					2,800	81	0.35	110	2.3	0.44
	6 7/8	1 3/8	1 3/8	1 3/8	1 3/8	1 3/8			6,400	311	0.69	955	61	0.87
	9 5/8	1 3/8	1 3/8	1 3/8	1 3/8	1 3/8	1 3/8	1 3/8	11,325	769	1.0	2,180	232	1.3
E4	4 1/8	1 3/8	1 3/8	1 3/8					4,525	115	0.53	180	3.6	0.63
	6 7/8	1 3/8	1 3/8	1 3/8	1 3/8	1 3/8			10,425	441	1.1	1,570	95	1.3
	9 5/8	1 3/8	1 3/8	1 3/8	1 3/8	1 3/8	1 3/8	1 3/8	18,400	1,090	1.6	3,575	360	1.9
V1	4 1/8	1 3/8	1 3/8	1 3/8					2,090	108	0.53	165	3.6	0.59
	6 7/8	1 3/8	1 3/8	1 3/8	1 3/8	1 3/8			4,800	415	1.1	1,430	95	1.2
	9 5/8	1 3/8	1 3/8	1 3/8	1 3/8	1 3/8	1 3/8	1 3/8	8,500	1,027	1.6	3,275	360	1.8
V2	4 1/8	1 3/8	1 3/8	1 3/8					2,030	95	0.46	160	3.1	0.52
	6 7/8	1 3/8	1 3/8	1 3/8	1 3/8	1 3/8			4,675	363	0.91	1,370	81	1.0
	9 5/8	1 3/8	1 3/8	1 3/8	1 3/8	1 3/8	1 3/8	1 3/8	8,275	898	1.4	3,125	309	1.6
V3	4 1/8	1 3/8	1 3/8	1 3/8					2,270	108	0.53	180	3.6	0.59
	6 7/8	1 3/8	1 3/8	1 3/8	1 3/8	1 3/8			5,200	415	1.1	1,570	95	1.2
	9 5/8	1 3/8	1 3/8	1 3/8	1 3/8	1 3/8	1 3/8	1 3/8	9,200	1,027	1.6	3,575	360	1.8

Figure 1.2 CLT Grades and Bending Properties (ANSI APA PRG 320)

CLT is made from a variety of dimension lumber species and grades. Some common examples include spruce-pine-fir as indicated earlier in Table 1. These lumber boards are stacked perpendicular to each other and attached together. Glue is typically used to attach the dimension lumber. Sometimes fasteners are also used, although this is less common (CLT Handbook, 2013). This results in a wood panel that has dimension lumber boards going in both the parallel and perpendicular directions (CLT Handbook, 2013). Figure 1.3 illustrates a few different sizes and views of small CLT panels.

Figure 1.3 CLT Panels

A CLT panel has at least three layers of lumber boards. The most commonly used CLT panels have three, five, or seven layers. The lumber boards are typically 0.625-inches to 2-inches thick and from 2.4-inches to 9.5-inches wide. The size of a CLT panel depends on the manufacturer and is typically restricted by transportation constraints or the size of the press used to make the CLT. They are available in widths of 2 ft., 4 ft., 8 ft. and 10 ft. and can be 60-ft. long in the United States, but less than 40 ft. in length is more typical for transportation. The thickness can be up to 20 inches (FPInnovations, 2013). Figure 1.4 shows a side view of CLT panels.

Figure 1.4 CLT Panels in the Laboratory at Colorado State University

1.2 Earthquakes

Earthquakes result in landslides, tsunamis, surface faulting, and ground shaking. They often lead to a loss of human life. On average, there are over 1,000 earthquakes worldwide annually with a number of them occurring around the so-called geographic Ring of Fire. Most of these are magnitude 5 or lower, which are not expected to cause structural damage in engineered buildings, nor in any buildings in developed countries. A few of these earthquakes are magnitude 7 or higher. They damage structures and other physical infrastructure, resulting in economic losses (EERI, 2003). The United States Geological Survey (USGS) website provides information on the occurrences, magnitudes, and resulting damage data for U.S. earthquakes. Figure 1.5 shows the largest earthquakes in the U.S. continental states.

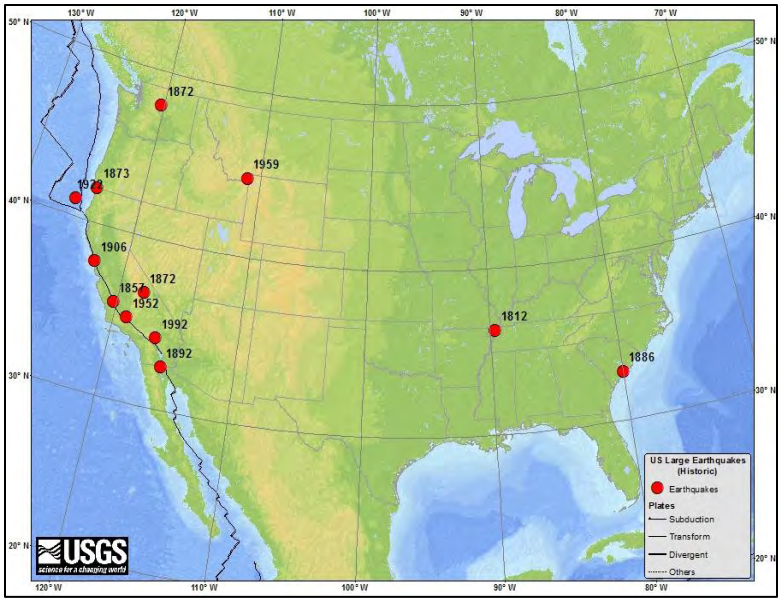

Figure 1.5 Largest Earthquakes in Contiguous U.S.A. (http://earthquake.usgs.gov/earthquakes/states/10_largest_us_maps.php#48_states)

1.3 Motivation

CLT was introduced to North America in the early 2000s. At that time, there were no guidelines on how to use CLT as a construction material. A comprehensive streamlined building code was not available nor any bridge deck design guidance for using this material. Because this was a new product, there were many practical challenges to the implementation of CLT in North America, such as material supply, serviceability, fire performance, structural safety, and code acceptance (Pei et al., 2016). The U.S. Edition of the CLT Handbook has provided researchers with useful information about CLT, but the lack of a recognized building code for CLT and no agreed upon design method leaves designers to use the alternative methods portion of the ASCE 7 standard (2016).

This report presents the results of a CLT diaphragm tested as a large cantilever. The primary reason to do this test was to observe and document the behavior of a CLT diaphragm under seismic loading that was designed using basic structural analysis, mechanics, and U.S. design standards (NDS, 2015). The results of the test were analyzed and conclusions provided with the intent of assisting in the development of design standards for CLT construction in the United States.

1.4 Literature Review

1.4.1 Introduction to Diaphragms

An engineered building designed for seismic load has what is known as a seismic force-resisting system (SFRS). The primary function of an SFRS in a building is to transmit loads from their origin (typically floor diaphragms or bridge decks) down to the supporting foundations. SFRS is a three-dimensional system that has different components. The horizontal components are primarily floors and roofs, which transmit the load to the vertical components. The vertical components are usually walls and frames. These transmit the loads from a floor or a roof either to the lower horizontal elements or to the foundations. The horizontal elements are diaphragms. Diaphragms also act as roofs and floors in a building and help resist gravity loads and wind uplift forces (Cobeen et al., 2014).

Figure 1.6 illustrates the components of a diaphragm.

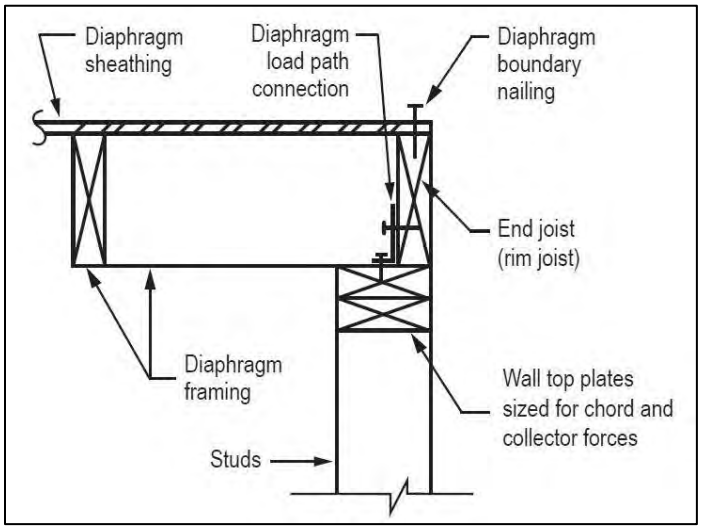

Figure 1.6 Components of a Diaphragm
(After Cobeen et al., 2014)

1.4.2 CLT Projects

The number of CLT construction projects in North America is on the increase. The wood Innovation and Design Centre was completed in 2014. This is a 96-ft., eight-story building in British Columbia and is the tallest contemporary wood building in North America. The Framework Project is a 12-story tall CLT building in Portland, OR, expected to start construction in January 2018. Carbon 12 is another building in Portland planned by PATH Architecture, Inc., and to be constructed by Kaiser Group, Inc. A few other notable projects to be built include 475 West 18th in New York City, the Hines T3 Project in Minneapolis, and the Arbora Complex in Montreal. There are a few other projects under planning (See Pei et al., 2016, for a complete listing).

1.4.3 CLT Research

The SOFIE project was conducted in Italy in early 2000s and was funded by the Trento province of Italy. A combination of shear wall tests, connection tests, and full scale building tests were conducted to enable a comprehensive study on the seismic performance of CLT construction. The U.S. Department of Agriculture (USDA) Forest Products Laboratory (FPL) funded a research project to complete a FEMA P-695 evaluation (FEMA, 2009) on CLT shear walls. Colorado State University is currently conducting this study, which has focused on testing of shear walls, nonlinear static and dynamic analyses, peer-review, design methods, and other methods with the goal of identifying seismic design parameters (Amini et al., 2016). This is to be in accordance with current U.S. codified design and eventually be adopted into ASCE 7. At the time of this work no CLT diaphragm testing had been done, either for buildings or bridges.

1.4.4 CLT Behavior

CLT diaphragms are mass timber diaphragms. The behavior of these mass timber diaphragms is usually influenced by strength, ductility, and the flexibility of connections between the CLT panels and the other components (Breneman, Jun 2016). The CLT panels making up the floor or the roof diaphragm are known to rotate as rigid bodies under in-plane loading (e.g., shear). Therefore, the focus is on the design and subsequent behavior of the panel connectors.

2. SPECIMEN DESIGN AND EXPERIMENTAL SETUP

2.1 CLT Design

To design a CLT bridge deck diaphragm one has to understand how CLT behaves. CLT panels are usually used as wall and floor/roof members. CLT panels can also be used for bridge piers or bridge decks. The design procedure depends on many factors. Short-term and long-term behavior is important. In-plane and out-of-plane stiffness, shear strength, and bending strength should be considered (FPInnovations, 2013).

2.2 CLT Diaphragm Design

The experiment used E1 category CLT panels, which are classified as 1950f-1.7E Spruce - Pine - Fir - MSR lumber in all parallel layers and No. 3 Spruce - Pine - Fir in all perpendicular layers (ANSI APA PRG 320).

Spickler et al. (2015) developed a white paper for guidance, and that example was applied for guidance in this experiment. The Standard Test Method for Static Load Testing of Framed Floor or Roof Diaphragm Constructions for Buildings (ASTM E455 -11) was used as a guideline to design and follow the test procedures. A cantilever beam diaphragm test with a concentrated load was conducted and, because it was a damaging test, only one major test was conducted as described later in this report.

The design process involves a pre-determined set of steps. The first step is to determine seismic load on the diaphragm. Checking the diaphragm aspect ratio and allowable in-plane shear capacity of the diaphragm are included in the second step. In the third step, panel-to-panel connections are designed and boundary conditions are assessed. The diaphragm chord members and their connections are designed in the fourth step. To conclude, diaphragm strength level deflection is calculated and the diaphragm flexibility assumption is verified (Spickler at al., 2015).

Ten pieces of E1 category CLT Panels were used to form the sheathing of the diaphragm. A couple of these panels were cut smaller than the others with dimensions approximately 7 ft. by 1.4 ft. The other eight panels were larger and their dimensions were 7 ft. by 3.75 ft. These panels were connected to each other by a set of steel splice connectors to form a butt joint as illustrated in the design drawings. These joints were in north-south directions.

2.3 CLT Diaphragm Test Setup

The diaphragm is set up as a cantilever beam and loaded horizontally as described later. Due to this setup, the shear and moment are developed in the diaphragm as shown in Figure 2.1

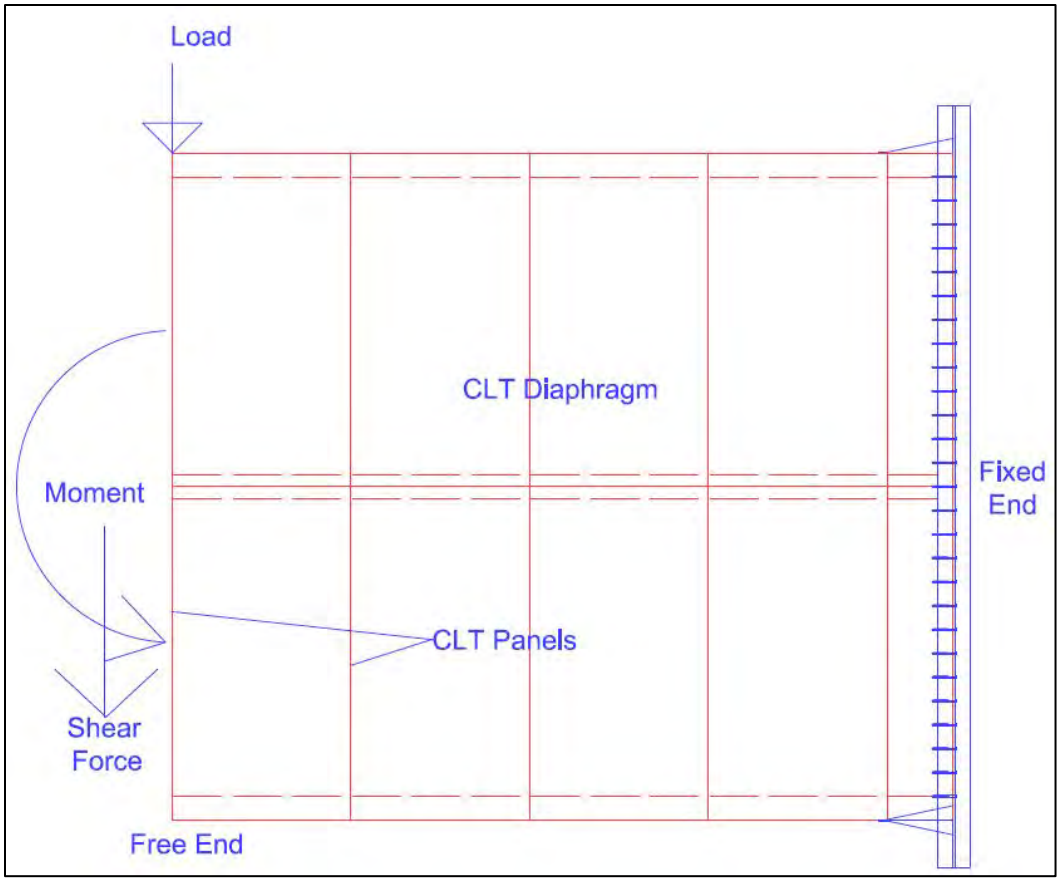

Figure 2.1 Cantilever Beam

Figure 2.2 shows the plan of the CLT diaphragm test setup. Actuator is in green. Wood is drawn in red and steel is shown in blue.

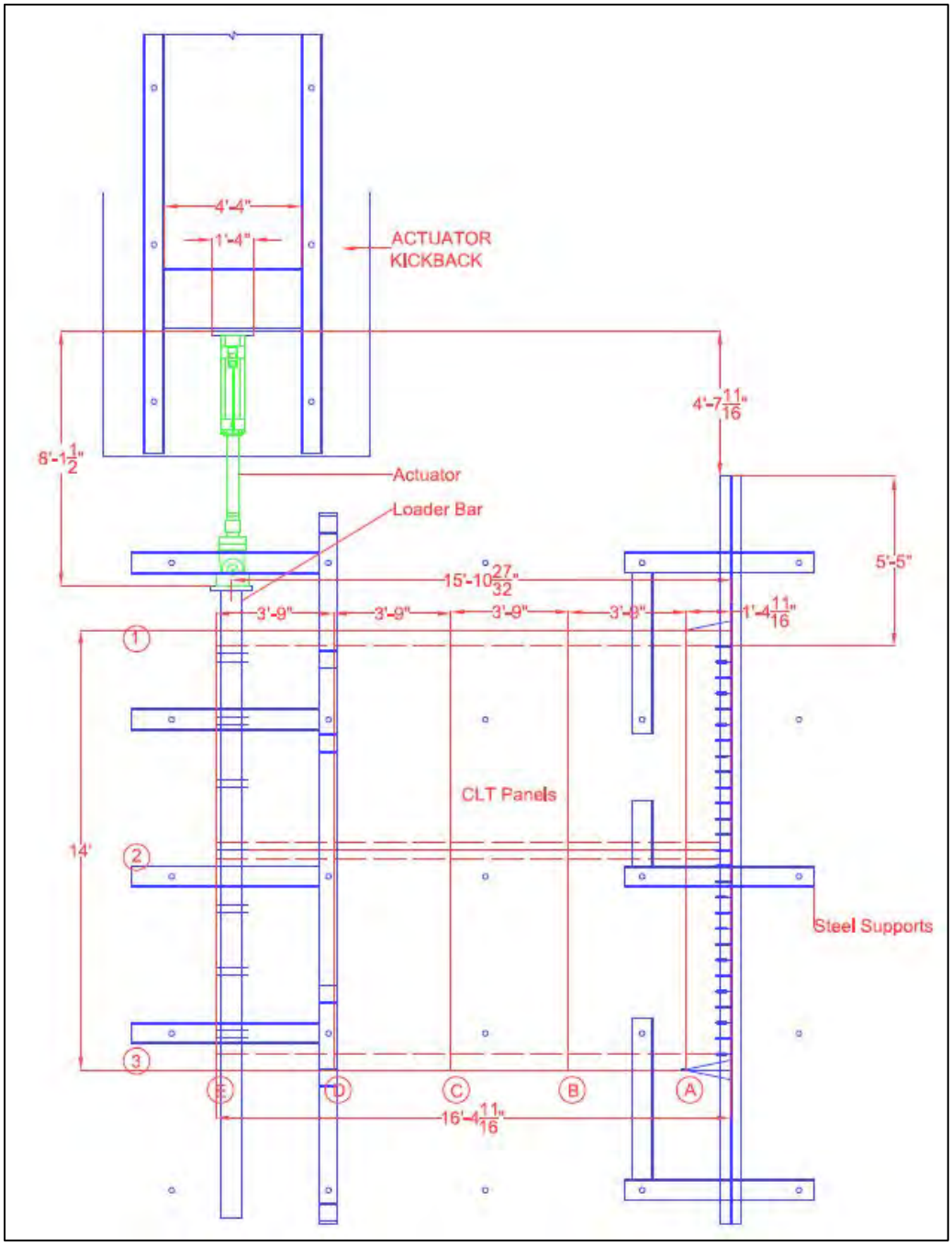

Figure 2.2 CLT Diaphragm Test Setup Plan View

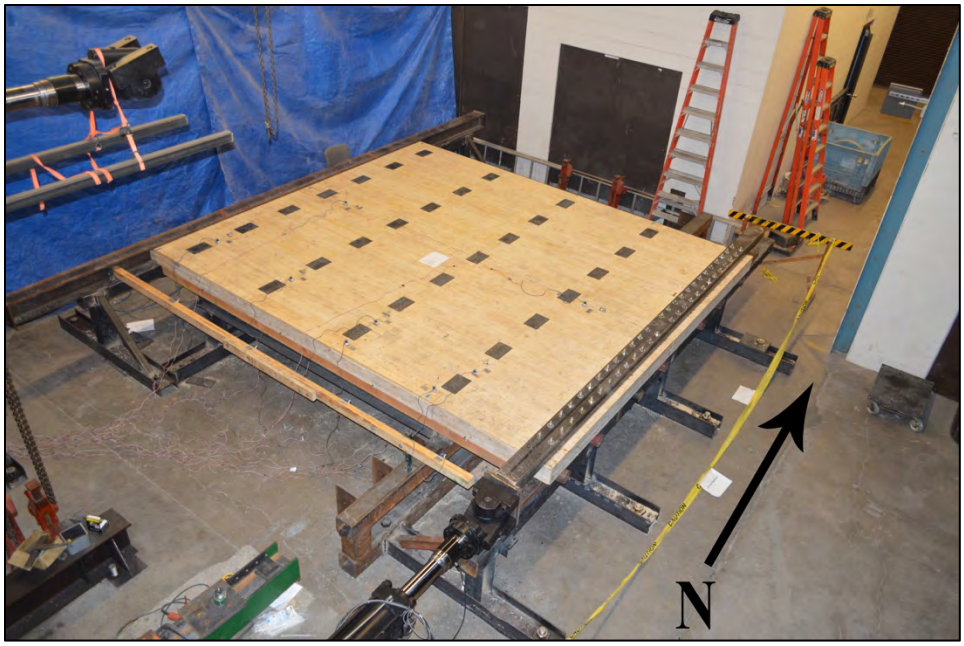

Figure 2.3 CLT Diaphragm Test Setup (View from a Top Angle)

Figure 2.3 shows a photo of the test setup from the top. The fixed end of the cantilever is on the west side of the test setup. A steel W-beam is connected to CLT panels 5 and 10 to form the fixed end. Holes are drilled through the web of the steel I-beam to make a fixed connection. The connection is made with lag screws that are drilled into the side grain of CLT panels. The SDS screw connection to the CLT panels from the top is shown in Figure 2.4. Figure 2.5 shows the rows of SDS screws drilled through the CLT panels. These SDS are 2.5-inches deep into the chord members underneath. This was done to ensure sufficient penetration for maximum strength.

Figure 2.4 SDS Screws into CLT

Figure 2.5 SDS Screws in a Line Connecting CLT to Chord Members

Figure 2.6 gives us a detailed look of different types of connectors used in the test setup. All the connectors are labeled and CLT panels are numbered for discussion of the test results.

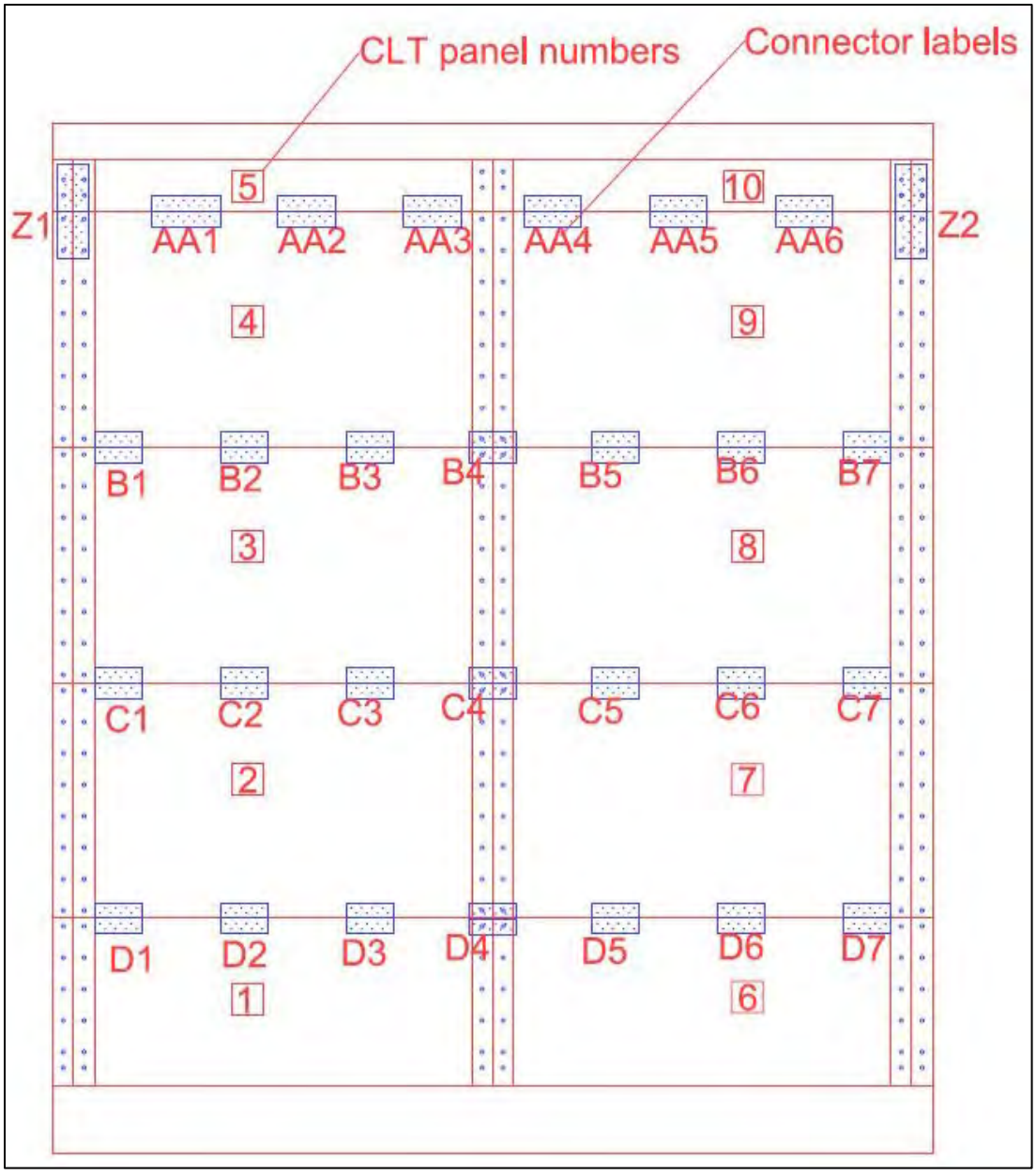

Figure 2.6 Connector Layout (Plan View)

Figure 2.7 West End Steel I-Beam

Figure 2.7 shows the heads of lag screws going through the web of the steel I-beam on the west side (fixed end of the cantilever) of the diaphragm. These lag screws are drilled into the side grain of the CLT panels. The steel beam and CLT panels are supported by tube steel that runs in the north-south direction under the steel I-beam. A frame supports this tube steel. The steel frame starts on the west side. The first components are set underneath the tube steel on the fixed end. These act as legs to connect the fixed end to the concrete strong floor. The steel frame is fixed into the concrete strong floor with the use of 2-inch threaded rods that have pre-drilled holes into the floor. The steel frame has kickbacks into the concrete floor. From this end, there are three long pieces of tube steel that span the length of diaphragm. These members are used to support the three chord members that support the diaphragm. The chord members are connected to the diaphragm with SDS screws.

On the east end underneath the chords and the supporting steel tubes, there is another set of legs that connect the diaphragm to the concrete strong floor. On the easternmost end of the test setup, these members connect to another steel frame. This steel frame has steel rollers on the top. These rollers are kept underneath the loader bar setup to reduce or eliminate any friction that would occur if it were sliding and allows the loader bar to move during testing. This is illustrated in Figure 2.8.

Figure 2.8 East End of the Test Setup

At the south end of the loader bar the actuator is connected to the loader bar. The actuator sits on a block of concrete. The actuator is mounted on a steel plate, which is connected to a steel beam that distributes the load into two steel beams that are placed into the strong concrete floor. At the end is another steel tube.

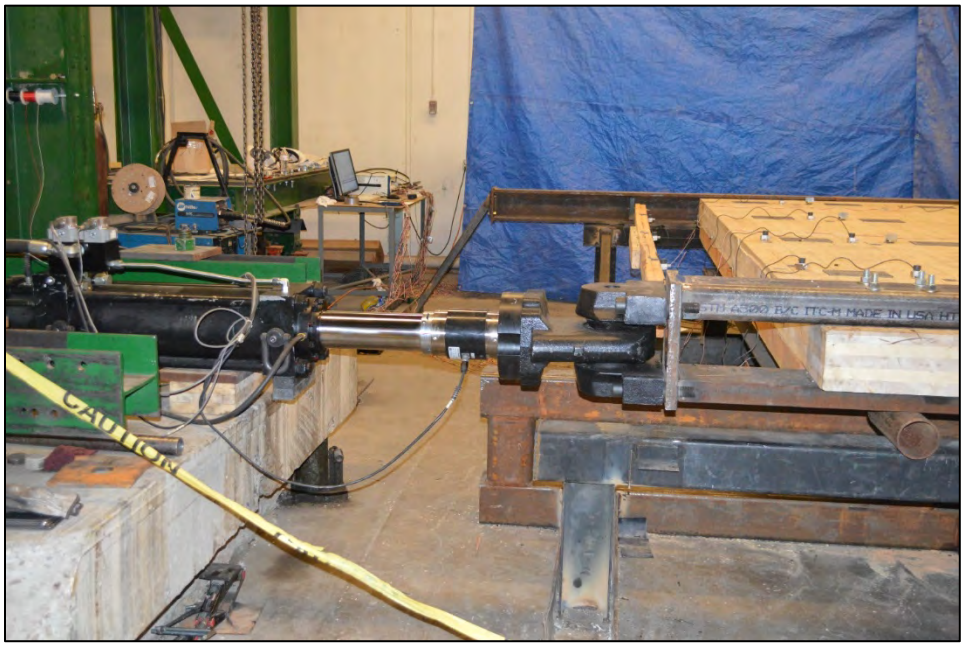

Figure 2.9 Southeast End of the Test Setup

Figure 2.9 shows the actuator connection to the loader bar. The concrete block underneath the actuator is also visible. This provides support and acts as a kickback to control the resistance from loading when testing the diaphragm. All the other necessary drawings and photos have been included in the Appendix of this report.

2.4 CLT Diaphragm Design

The design procedure for a CLT diaphragm consists of five distinct steps. First the wind/seismic load acting as the diaphragm is to be determined. Then the diaphragm aspect ratio is to be calculated and allowable panel in-plane shear capacity is determined. The panel-panel connections and boundary conditions are designed. Then the chord members and their connections are designed. In the last step, the diaphragm deflection is calculated and the flexibility assumption is verified.

The diaphragm is approximately 16-ft. long and 14-ft. wide. The aspect ratio was calculated.

Diaphragm Aspect Ratio
L/W ~ 16'/14' ~ 1.143 < 4.0

The seismic load in this experiment was applied by an actuator. The design load was assumed to be 16 kips. From this the shear load along line A was calculated. Then the ASD design load was calculated according to ASCE guidelines.

Seismic Load (from Actuator)

Assume W_{EQ} = 16 kips

Line A V_{EQ} = 16000lbs

V_{EQ} = (16000/14') = 1142.857 plf

ASD Design Load
= (0.7)*(V_{EQ}) = 800 plf

The CLT panels used are E1 category. The specifications are as follows:

E1 Category CLT 1950 f – 1.7E

Spruce – Pine – Fir – MSR lumber in all parallel layers and No 3. Spruce – Pine – Fir in all perpendicular layers

For inter-panel connections, steel splices were used. 10 gage steel was used. 16d common nails were used. The connectors along lines B,C,D,E were different from the connectors along line A.

Panel – Panel Connection (lines B,C,D,E) (Connectors A,B,C,D)

10 gage steel splice with 16d common nails

C_D = 1.6	NDS-2015 Table 2.3.2
C_{di} = 1.1	NDS-2015 Section 12.5.3
Z = 139 lb/nail	NDS-2015 Table 12P
Z' = (1.6)*(1.1)*(139) = 222.4 lbs	NDS-2015 Section 12.3.1
Required spacing = (222.4)*(12)/800 = 3.336"	
Minimum nail spacing = 15d = (15)*(0.162) = 2.43"	NDS-2015 Table C 12.1.1.66
Use 2.5" spacing	

8 nails on one side
Total capacity per splice= 8*222.4 = 1779.2 lbs
Use 7 splices
Total Splice Connection Capacity = 12454.4 lbs

Panel – Panel Connection (Line A)(Connectors AA)

Use 16 nails on one side, Use 6 Splices
Total Splice Connection Capacity = 21350.4 lbs

Tension plates were used on the fixed end of the diaphragm. 10 gage steel plate was used with SDS screws.

Tension Plate Design (Connectors Z)

Unit Shear of metal connector with approx. 2' spacing
Moment Arm = 16.39'
Tension Force = 16.39*650 = 10653.5 lbs
Approx. number of SDS screws on each side = 10653.5/(420*1.6) = 15.85 ~ 16 screws on each side of 10 gage steel plate

Chord members were designed next. The moment was calculated and then chord forces were determined.

Diaphragm Chords

Moment at fixed end (Line F) = 262250 lb-ft
Chord force = M/d
Assume d = [(14)*(12)]/12 =14' (No walls on either end)

Strength Level Chord forces

@ fixed end = 18732.14 lbs

ASD Chord forces

@ fixed end = (0.7)*(18732.14) = 13112.5 lbs

Tension Capacity

F_{T0} = 1375 psi — APA PRG 320 Table A1 for Grade E1
C_D = 1.6 — NDS-2015 Table 2.3.2
F'_{T0} = (1.6)*(1375) = 2200 psi

After calculating the tension capacity, SPF dimension lumber was decided to be used.

Use 4 x 8 chord members
SPF Dimension Lumber 4 x 8 member
F_t = 700 psi Table 4A NDS-2015 Supplement
$F_{c\perp}$ = 425 psi Table 4A NDS-2015 Supplement
$F_{cPARALLEL}$ = 1400 psi Table 4A NDS-2015 Supplement
Okay.

Then the tension capacity of the chord was compared to the tension load to ensure the designed chord member can sustain the load.

$F_T = F_t * A_{chord}$
$F_T = 700 * 3.5 * 7 = 17150 > 13112.5$
Okay.

The total tension capacity of the diaphragm was checked.

$A_{PARALLEL} = 3*1.375*8 = 33$ in^2 CLT Handbook Chapter 3 Section 2.3
(Area of layers with fibers running parallel to the direction of the load)
$A_{NET} = 33$ - (2 screws)*(0.228 shank diameter)*(3.54 length - 0.25 tip) = 31.49 in^2
$T_{PARALLEL} = (2200)*(31.49) = 69278$ lbs > (13112.5)*(1.07) = 14030.375 lbs

Then the bending was checked.

Bending
W_{DL} = 20.125 psf (self weight) + 4.875 psf (DL) = 25 psf
M_{ALLOW} = 11250 lbs-ft APA PR L 314 (Feb 20, 2014)
$M_{DL} = (W*L^2)/8 = 839.5$ lbs-ft

Bending and Axial Tension

= (14030.375/69278) + (839.5/(1.6*11250)) NDS-2015 Eq 3.9.1
= 0.2025 + 0.0466 Section 3.9 Commentary
= 0.2491 < 1.0 O.K

The compression loading values were checked according to CLT handbook specifications. Combined bending and compression values were also checked.

Compression

Unbraced Length = 196.6875”
$EI_{eff,0} = 440*10^{\wedge 6}$ lbf-in^2/ft ANSI/APA PRG 320-2011
$GA_{eff,0} = 0.92*10^{\wedge 6}$ lbf/ft Standard for Performance Rated CLT
$F_{C,0}$ = 1800 psi Table A1
K_S = 3.6 CLT Handbook Chapter 3 -Table 2
NDS-2015 Table 10.4.1.1
$EI_{app} = (EI_{eff})/(1+ (K_s*EI_{eff})/(GA_{eff}*L^2))$ CLT Handbook Chapter 3 - Equation 5
$EI_{app} = 421.252*10^{\wedge 6}$ lbf-in^2/ft
$EI_{app\text{-}min} = 0.5184*EI_{app} = 218.377*10^{\wedge 6}$ lbf-in^2/ft CLT Handbook Chapter 3 - Equation 8
$P_{CE} = ((\pi^2)*EI_{app\text{-}min})/L_e^2 = 55712.57$ lbs/ft
$C_D = 1.6$
$P_C^* = F_{C0}*C_D*A = (1800)*(1.6)*(3)*(1.375)*(12\text{”width}) = 142560$ lbs/ft
$C_P = (1+(P_{CE}/P_{C*}))/2C - (((1+(P_{CE}/P_{C*}))/2C)^2 - (P_{CE}/P_C)/C)^{\wedge}0.5$ C = 0.9 for CLT
$C_P = 0.369$ CLT Handbook Section 2.2.2
$P_{ALLOW} = C_P*F_{C0}*C_D*C = 52604.64$ lbs
P_{ALLOW} Total = (52604.64)*(6/12) = 26302.32 lbs
P_{CE} = (55712.57)*(6/12) = 27856.29 lbs/ft

Combined Bending and Compression

$(P/P_{allow})^2 + (M/(M_{allow}(1 - (P_C/P_{CE}))))$
$= 0.5705$

3. TEST PROGRAM

3.1 Test Protocol

The Consortium of Universities for Research in Earthquake Engineering (CUREE) developed a loading protocol for testing of wood shear walls and other wood components and subassemblies as part of the CUREE-Caltech Woodframe Project (Krawinkler et al., 2001). Deformation controlled quasi-static cyclic testing was done. The cyclic load test typically follows the protocol shown in Figure 3.1.

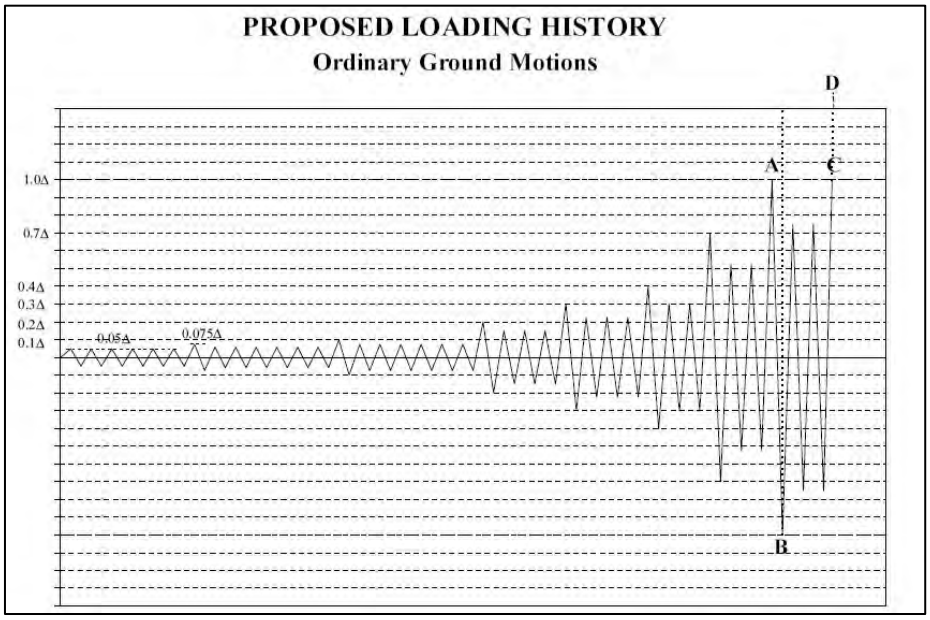

Figure 3.1 Loading History for Basic Cyclic Load Test
(Excerpted from Krawinkler et al., 2001)

The maximum displacement the test specimen can handle without total failure is called the reference displacement. The maximum displacement is usually determined by running a monotonic test. After doing a monotonic test, the monotonic displacement capacity Δ_m is determined. When the applied load drops to below 80% of the maximum load for the first time, the displacement is measured. This is the monotonic displacement capacity Δ_m. Then a factor of γ (typically 0.6) is multiplied with Δ_m to get the reference displacement Δ. $\Delta = \gamma * \Delta_m$. This is shown in Figure 3.2. Depending on the test some additional considerations should be taken into account (Krawinkler et al., 2001).

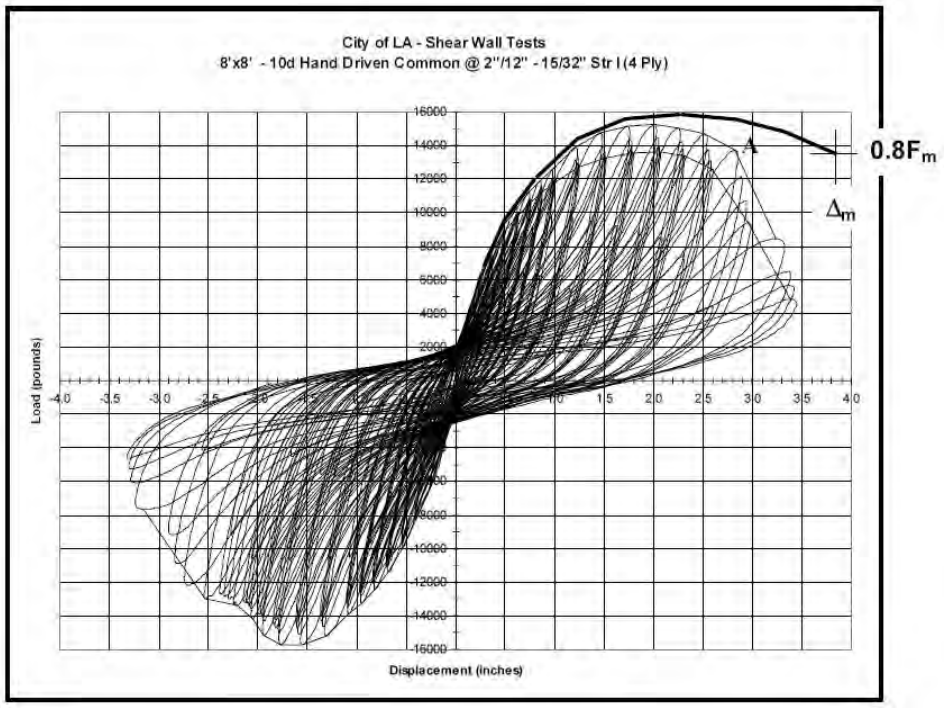

Figure 3.2 Δ_m (Monotonic Deformation Capacity) and its Relation to a Cyclic Test (Krawinkler et al., 2001)

Reference Deformation Δ is used as a measure of deformation amplitude. The loading history is developed by changes in the reference deformation Δ. It consists of three kinds of cycles. They are initiation cycles, primary cycles, and trailing cycles. The initiation cycles are very small in magnitude and are to make sure everything is running properly. If there is any problem, we can stop the test before we damage any of the equipment or the test specimen. Primary cycles are those that are larger than all the previous cycles. Primary cycles gradually increase the deformation to the reference deformation value. These are followed by smaller cycles, which are called trailing cycles. The amplitude of the trailing cycles is 75% of the amplitude of the previous cycles. All the cycles have the same magnitude in the positive and negative directions. CUREE has developed a sequence of cycles that should be executed as defined by the protocol, and Table 3.1 gives the details for this sequence.

Table 3.1 CUREE Test Protocol Sequence

Type of Cycle	**Number of Cycles**	**Amplitude (%Δ)**
Initiation Cycles	6	5
Primary Cycle	1	7.5
Trailing Cycles	6	5.625
Primary Cycle	1	10
Trailing Cycles	6	7.5
Primary Cycle	1	20
Trailing Cycles	3	15
Primary Cycle	1	30
Trailing Cycles	3	22.5
Primary Cycle	1	40
Trailing Cycles	2	30
Primary Cycle	1	70
Trailing Cycles	2	52.5
Primary Cycle	1	100
Trailing Cycles	2	75
Increasing steps of the same pattern with an increase in amplitude of 50%		

3.2 Test Instrumentation

Thirteen string potentiometers were used to measure a variety of parameters. These devices are a type of transducer. They are used to measure displacement and linear velocity. String potentiometers are also called string pots. A photo of a string pot is shown in Figure 3.3.

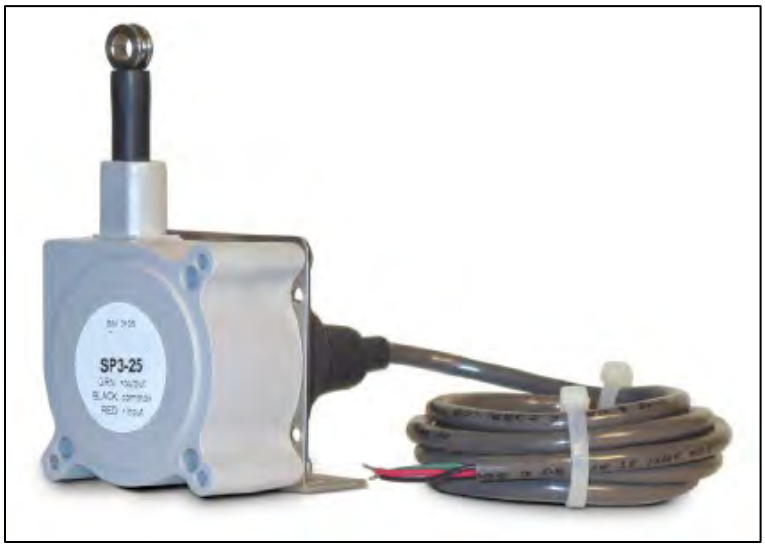

Figure 3.3 String Pot SP 3-25
(https://www.spectotechnology.com/product/string-potentiometer/)

Four of the string pots are used to measure linear deflection in the CLT panels with respect to actuator displacement. They are placed on the south side of the diaphragm into the panels. These are labeled 1, 2, 3, and 4. Figure 3.4 shows the locations of all the string pots in a plan view.

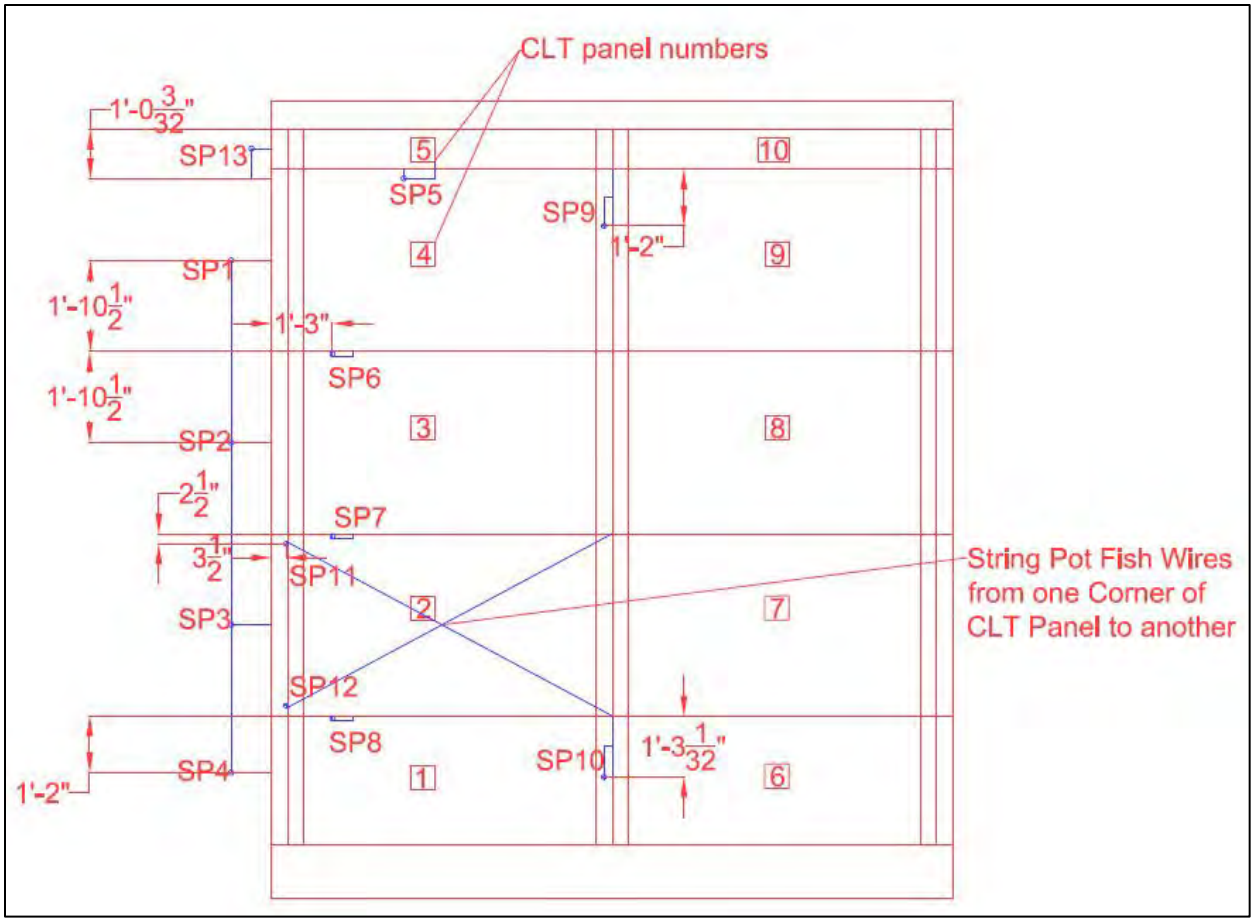

Figure 3.4 String Pot Locations on the CLT Diaphragm (Plan View)

String pots 5, 6, 7, and 8 were used to measure the twist between CLT panels in the north-south direction by placing them at the edge between panels. Similarly, string pots 9 and 10 measure twist in the east-west direction. Figures 3.5 and 3.6 show string pots 1 and 5 after installation.

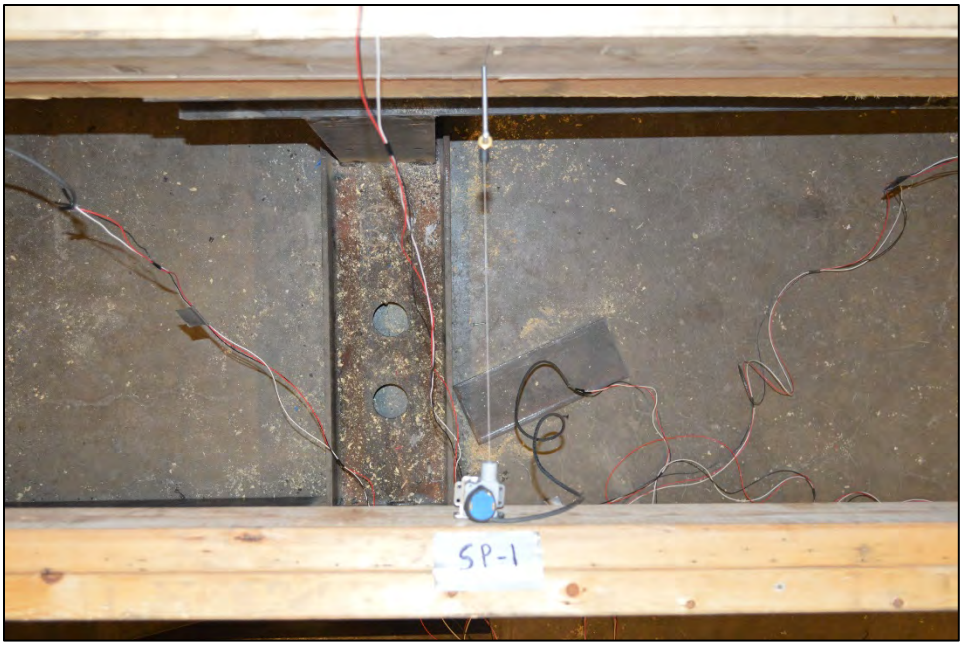

Figure 3.5 String Pot 1 Top View

Figure 3.6 String Pot 5 Top View

Figure 3.7 String Pot 10 Top View

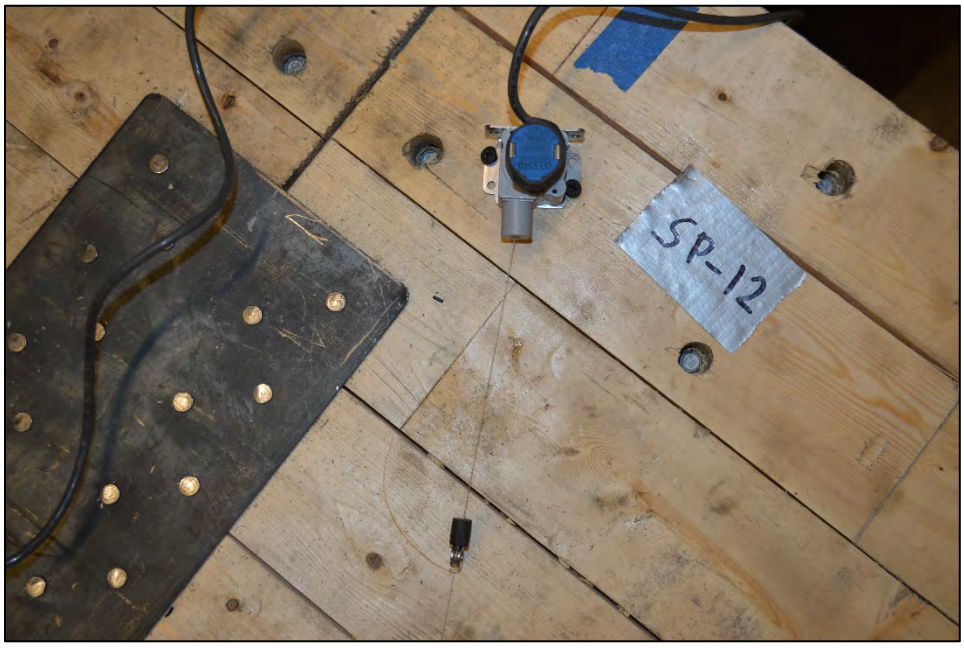

Figure 3.8 String Pot 12 Top View

Photos of string pots 10 and 12 after installation are shown in Figures 3.7 and 3.8.

String pots 11 and 12 were connected to fishing line and placed on top and diagonally across a single CLT panel. These string pots were used to determine if each panel acts as a rigid body and measure any shear deformation within the panel.

String pot number 13 was placed on the south side of the diaphragm on the edge of the CLT panels with the objective of measuring the separation between panels 4 and 5.

3.3 Testing

A total of four tests were conducted. All the tests were cyclic loading with the CUREE protocol described earlier, operating in displacement control. The first test had a reference displacement of 0.5 inches. The reference displacement for the second test was 1 inch. The third test was run until failure of the CLT diaphragm with a reference displacement of 6 inches. During the third test there was a tension failure in the connectors along line E. Because of this type of failure, the design of the diaphragm was modified for the final and most meaningful test of the program. The fourth test was run with a reference displacement of 3 inches based on knowledge gained from the previous three trial tests. The fourth and final test results are the focus of the remainder of this report and reflected in section 2.4.

4. TEST RESULTS AND DISCUSSION

4.1 Test Results

The failure of the diaphragm occurred on line B. This was in between panels 3 and 4 and 8 and 9. The failure occurred due to tension in the chord members. This tension force was transferred into the diaphragm through the SDS screws. An increase in the tension resulted in failure of the SDS screws in shear. This led to a small separation between CLT panels on either side of line 2. As the actuator displacement increased, the tension was being carried by the steel connectors. The cyclic loading protocol created a to-and-fro motion of the free end of the diaphragm. This led to increased separation along line 2. The nails holding the steel connectors that were along line 2 were pulled out of plane and started to fail in shear. It is illustrated in Figure 4.1.

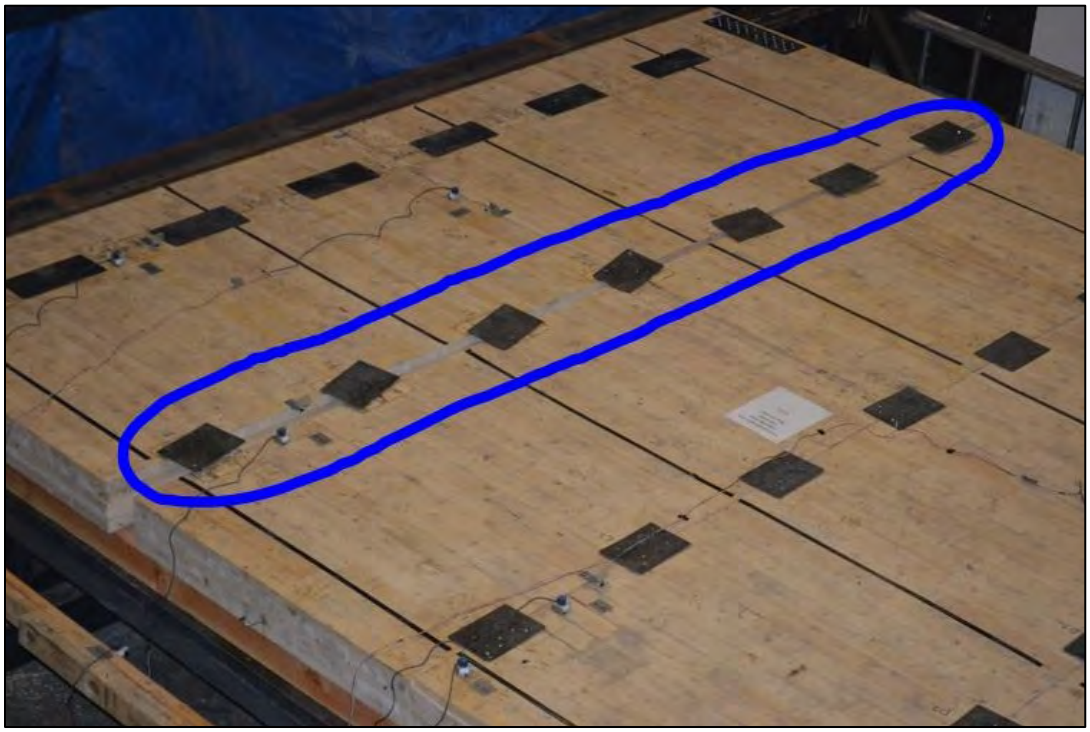

Figure 4.1 Failure Along Line B on the CLT Diaphragm

This behavior occurred because line A connecting panels 4 to 5 and 9 to 10 to the fixed end is designed as a part of the fixed end. HDU hold-downs were used to strengthen the connection in tension. This makes line A the fixed end of the cantilever. Therefore, when the SDS screws failed in shear and the CLT panels were separated from the chord members, the steel splices started to fail and the gap was created between panels. This is illustrated in Figure 4.2.

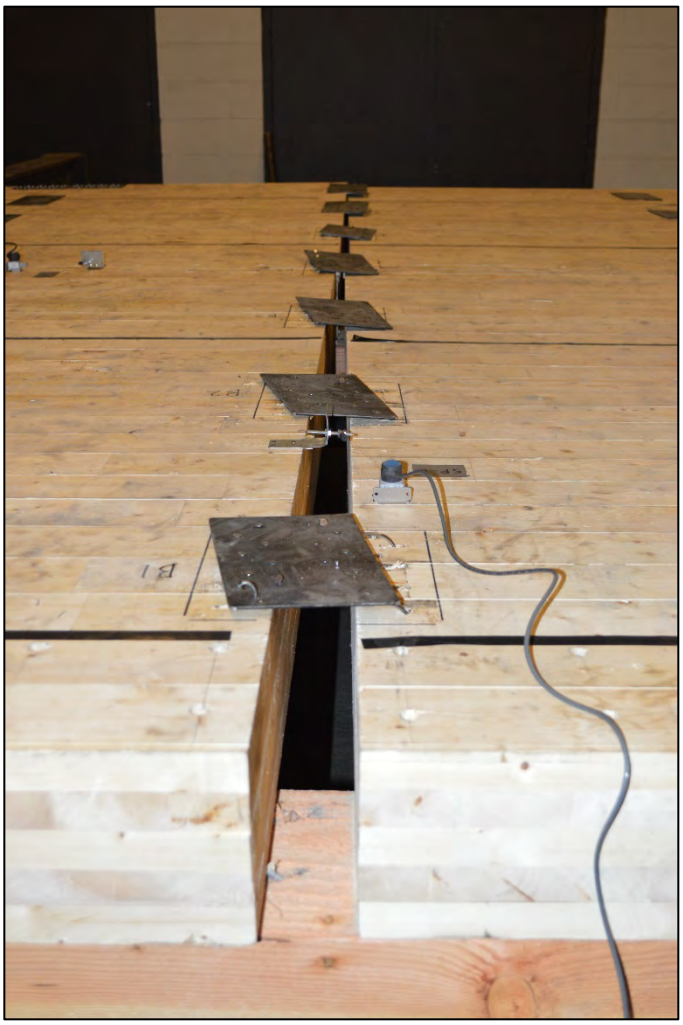

Figure 4.2 Failure Along Line B

Due to cyclic loading, the separation between panels kept gradually increasing with the increase in actuator displacement as expected. This resulted in shear failure of SDS screws in the chord underneath the diaphragm and subsequent failure of the steel connectors. As one can see in Figures 4.3 and 4.4, the panels separated and the gap between the panels increased from less than 0.25 inches to more than 3 inches prior to stopping the protocol.

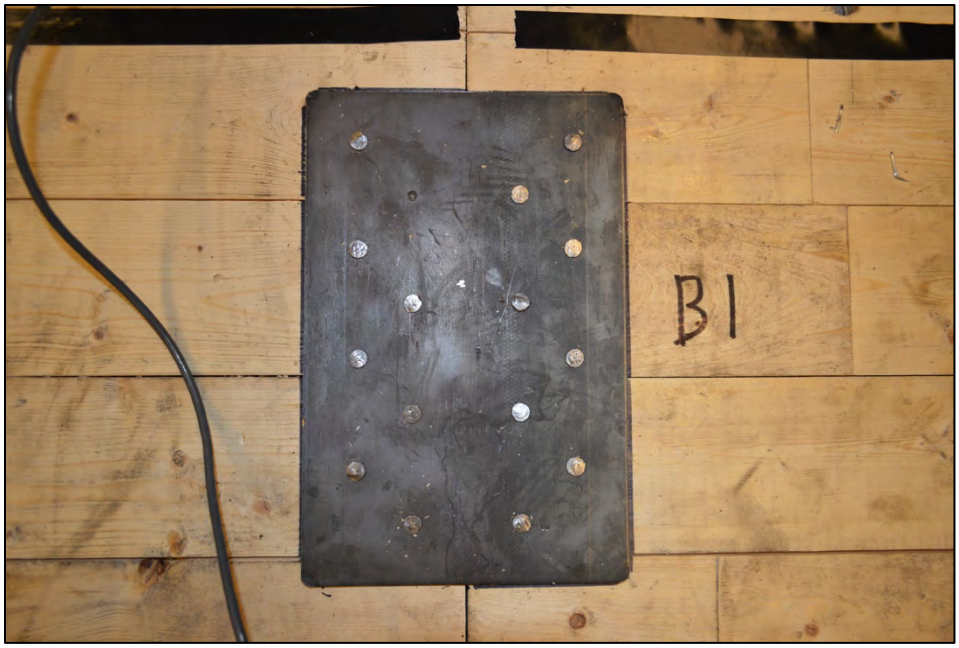

Figure 4.3 Gap between CLT Panels 3 and 4 before the Test

Figure 4.4 Gap between CLT Panels 3 and 4 after the Test

The steel splices started to fail gradually when in cyclic loading. First, the nails started to pull out slowly because of the in-plane movement of the CLT panels. Several nail heads sheared off because of the in-plane movement. As you can see from the following photos, there was total failure of the connectors along line B. Figure 4.5 shows connector B1 before the test.

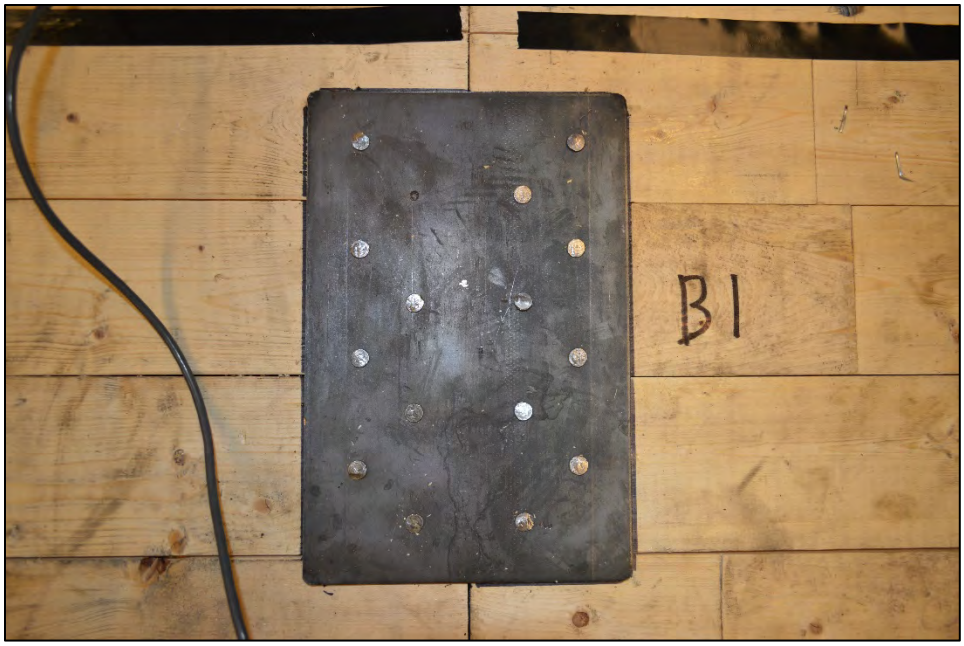

Figure 4.5 Connector B1 before the Test (Top View)

After the test, connector B1 had moved in all three directions. In Figure 4.6, one can see the black outline of a marker around connector B1, which was the original location of the B1 connector. It was twisted and turned due to cyclic loading. In Figure 4.7, we can see B1 did move out-of-plane because of the cyclic movement of the CLT panels. This type of failure occurred in all connectors on line B. More photos are included in the Appendix.

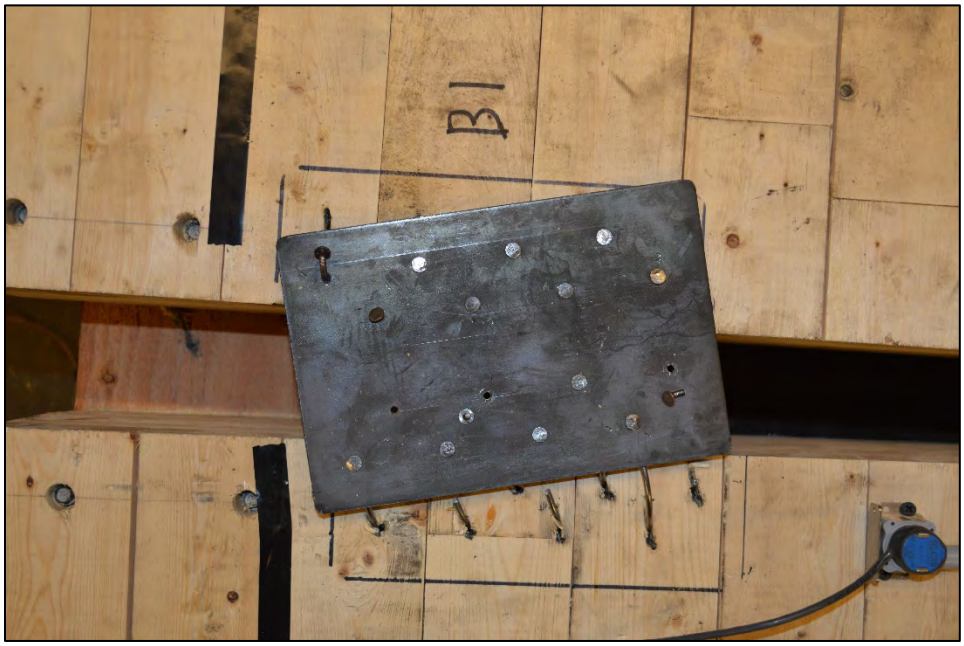

Figure 4.6 Connector B1 after the Test (Top View)

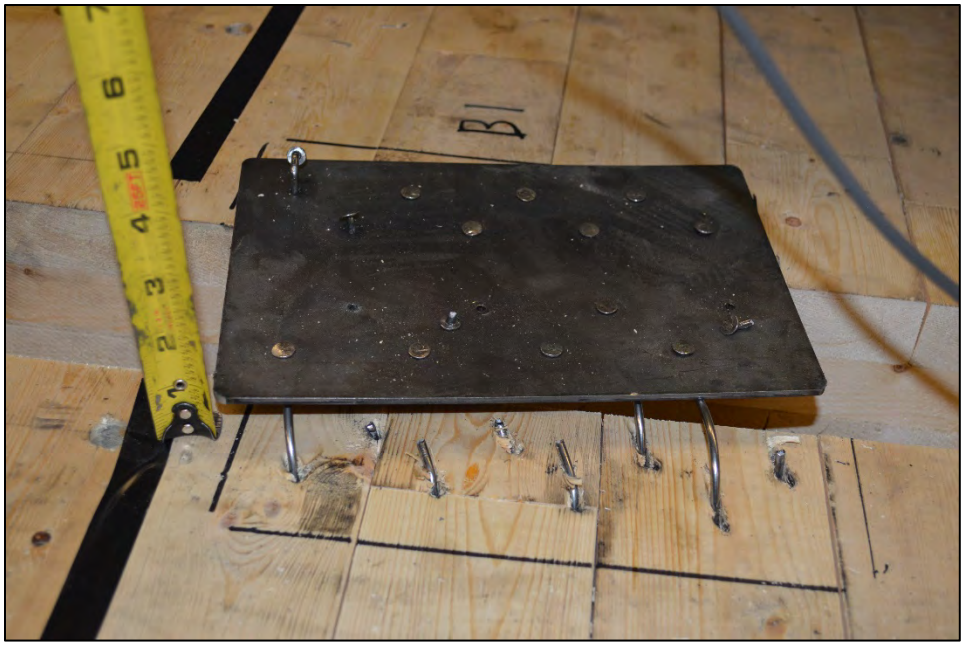

Figure 4.7 Connector B1 after the Test (Side View)

Figure 4.8 SDS Screw Shear Failure

In Figure 4.8, one can see the side view of CLT panels 8 and 9 and the chord member underneath. Failure of the SDS screws in shear can also be seen in Figure 4.8. CLT panel 9 has some slight wood crushing. This is due to panels pushing at each other because of the cyclic movement of the panels. This can be seen in Figure 4.9.

Figure 4.9 Wood Failure

4.2 Test Data and Discussion

String Pot number 2 malfunctioned and did not record data. The other 12 string pots recorded data as planned. For each of the string pots, time versus displacement is shown; although time is irrelevant it provides a measure against which to plot. In Figure 4.10 one can see the actuator displacement versus time plot, which had a maximum displacement of approximately 7.2 inches.

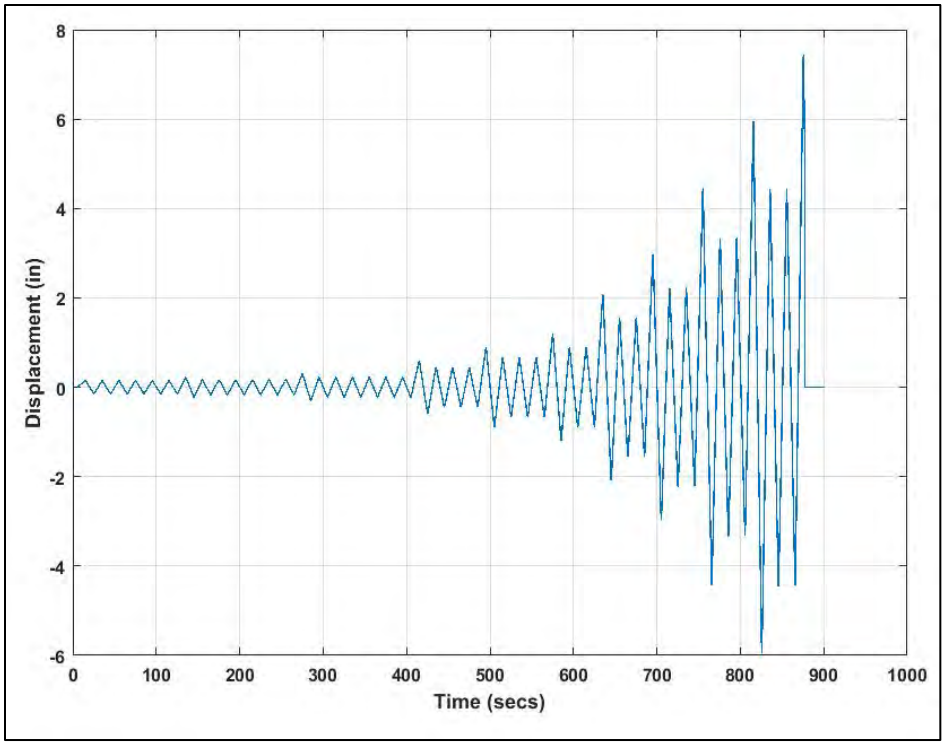

Figure 4.10 Actuator Displacement vs Time

As one would expect from basic beam theory, there is an increase in displacement as we move from the fixed end of the cantilever to the free end. SP4 was closest to the free end of the cantilever beam and SP1 closest to the fixed end. Figures 4.11 and 4.12 show the comparison between actuator and string pot displacements. In Figure 4.10, the difference in values between actuator and SP1 is approximately 6.5 inches at maximum actuator displacement. One can see there was very little deflection as one moves closer to the fixed end of the diaphragm. However, in Figure 4.12, one can notice the very similar plotlines of actuator and SP4. The difference in values was minimal. The slight lag was noted and was not intentional.

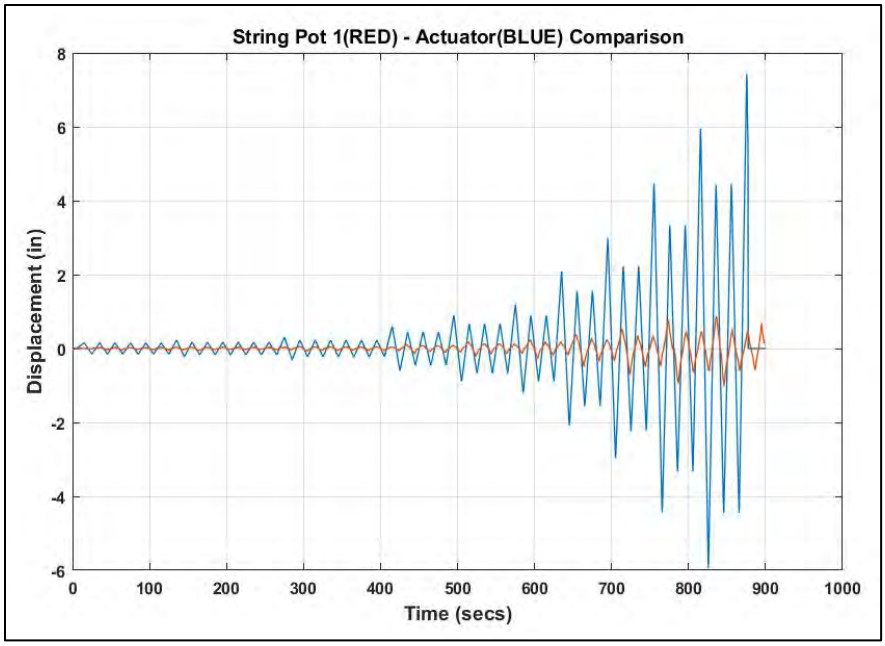

Figure 4.11 Actuator vs SP1 Data Comparison

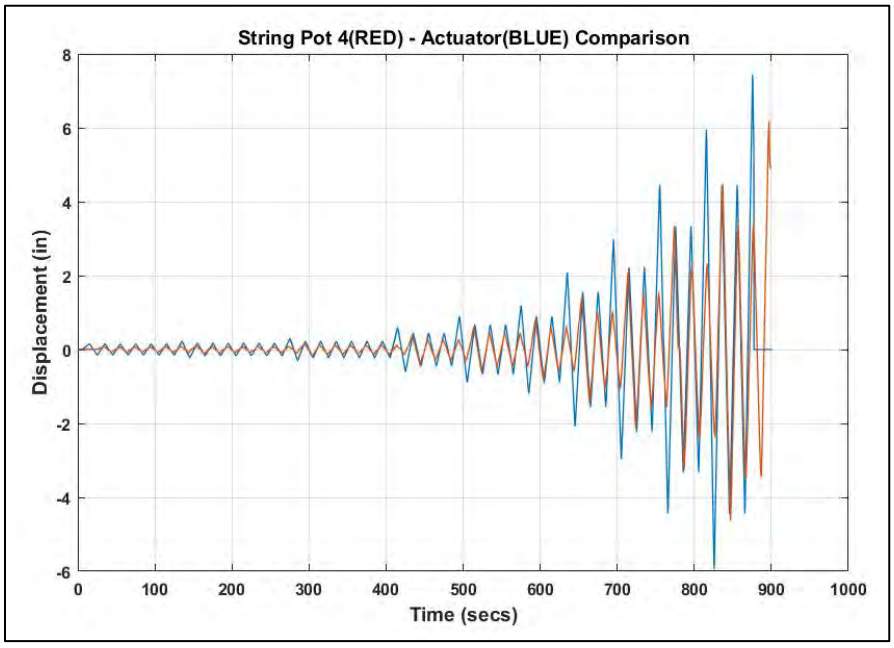

Figure 4.12 Actuator vs SP4 Data Comparison

Figures 4.13 and 4.14 compare data among SP1, SP3, SP3, and SP4. From the graphs, we can see that SP1 and SP3 have a large difference in values. However, SP3 and SP4 have almost indistinguishable values. This is because SP3 and SP4 are located very close to each other. SP1 is closer to the fixed end and far from SP3 and SP4.

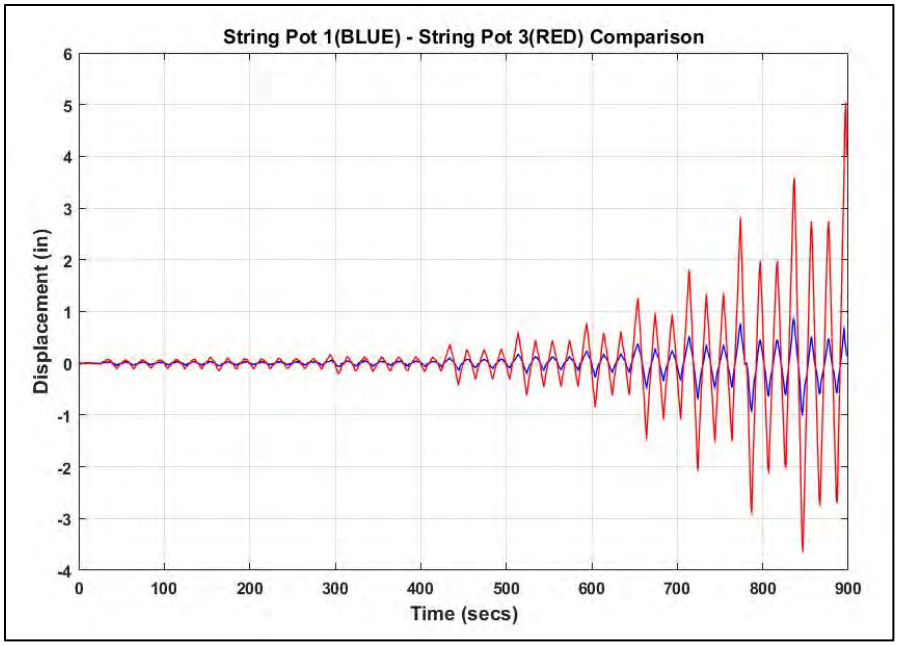

Figure 4.13 SP1 vs SP3 Data Comparison

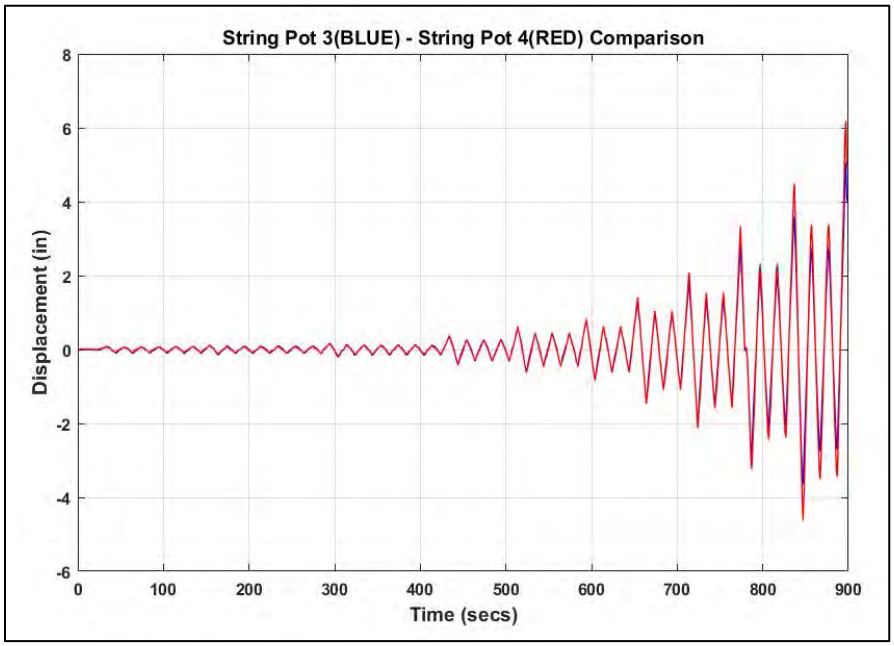

Figure 4.14 SP3 vs SP4 Data Comparison

SP5, PS6, SP7, and SP8 showed similar plot curves. SP6 has higher displacement values because it was on the line of failure. SP5 has slightly lower values. SP7 and SP8 are farther from the line of failure but have high displacements because they are closer to the free end of the cantilever.

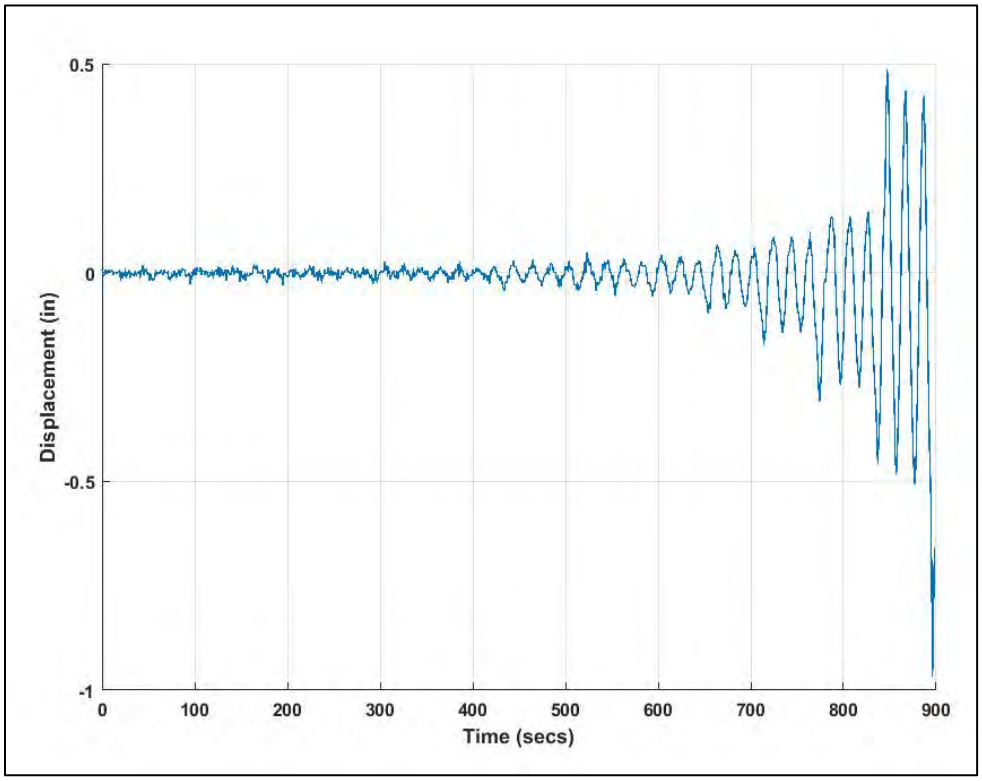

Figure 4.15 SP6 Data

The data from SP6, which are plotted in Figure 4.15, show us when failure occurred and the separation that was created between panels 3 and 4. The failure occurs when the displacement is approximately 0.3 inches. The actuator displacement was approximately 4 inches. After the initial failure occurred, the displacement values keep increasing with every cycle, resulting in total failure. SP7 and SP8 data are plotted in Figures 4.16 and 4.17.

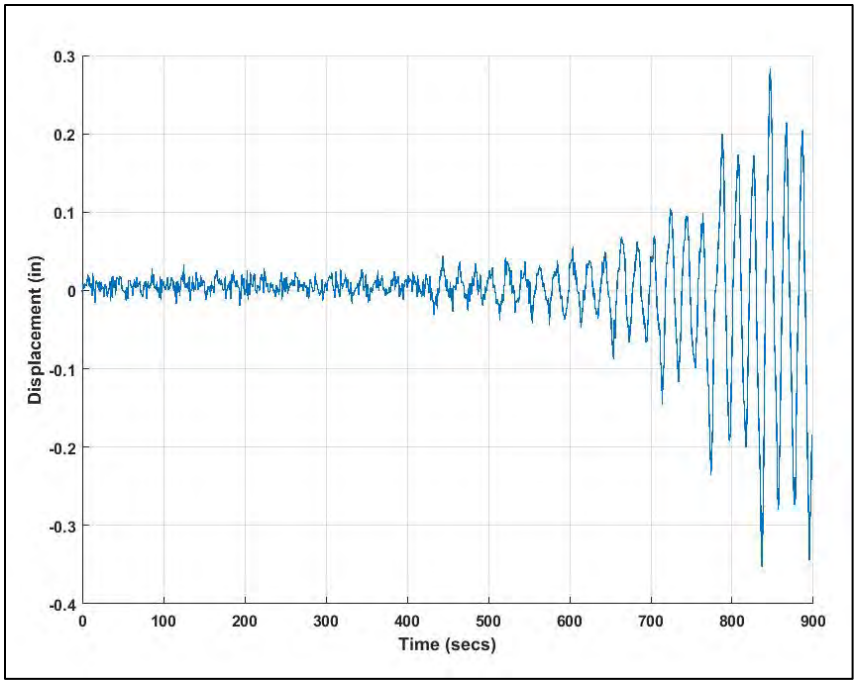

Figure 4.16 SP7 Data

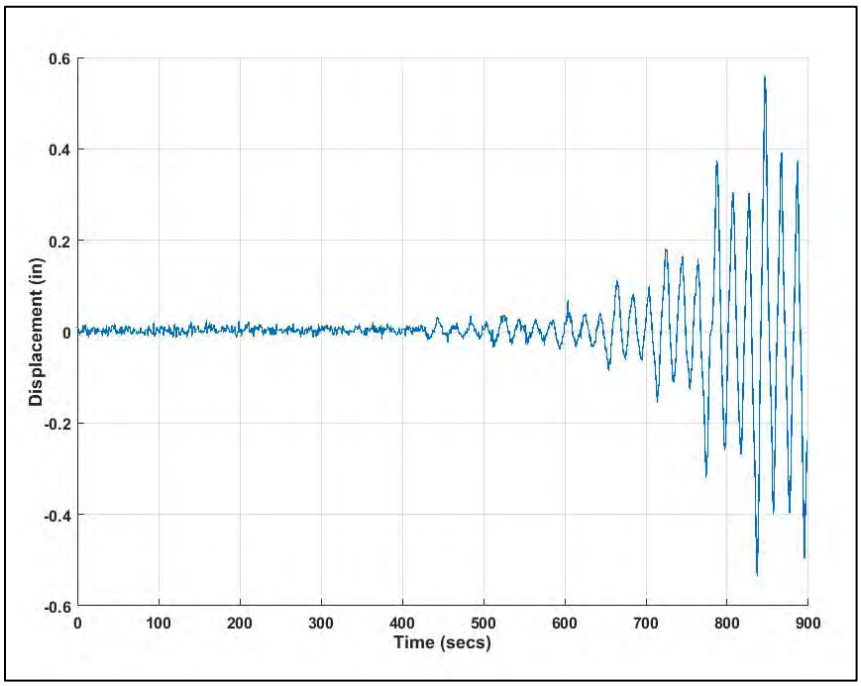

Figure 4.17 SP8 Data

Figure 4.18 shows a plot of data from SP9, which gives us the separation among panels 1, 2, 3, 4, 5 and 6, 7, 8, 9, and 10 on the west end. The displacement values were low and then there was a steep increase. The tension load transferred to steel splices due to the failure of chord member connections. The separation then increased due to the cyclic movement of the diaphragm.

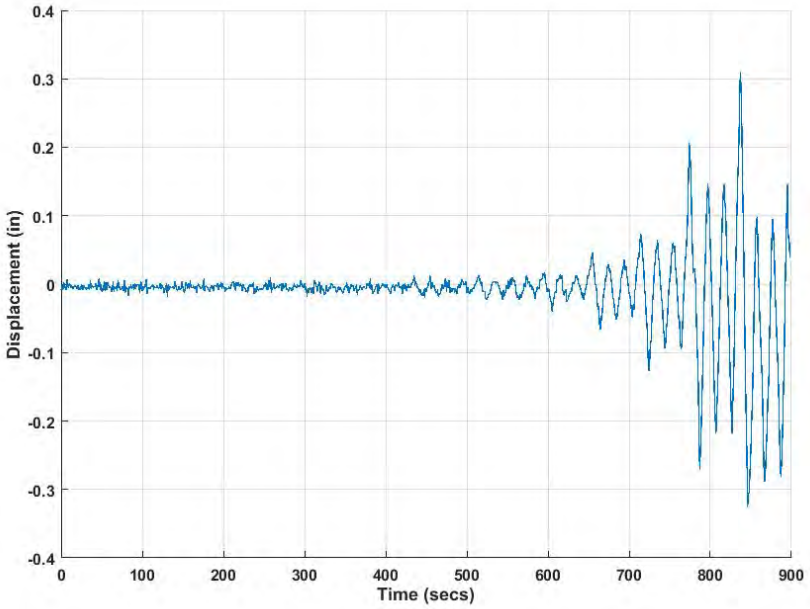

Figure 4.18 SP9 Data

SP10 gives us the separation among panels 1, 2, 3, 4, 5 and 6, 7, 8, 9, and 10 on the east end. SP10 is closer to the free end, but it is farther from the line of failure and it measures separation in the north-south directions. Therefore, it has very low values. This is illustrated in Figure 4.19.

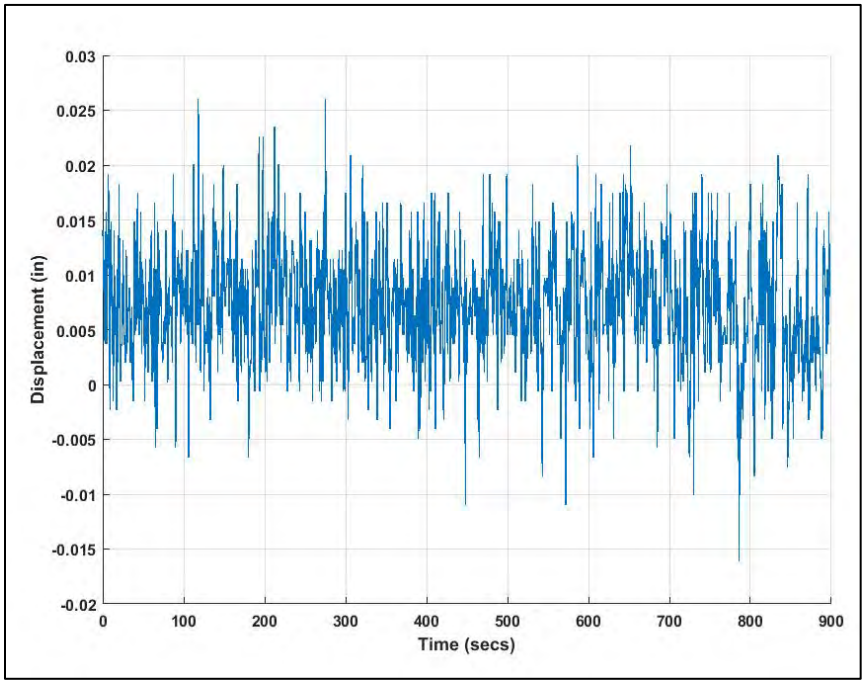

Figure 4.19 SP10 Data

Figures 4.20 and 4.21 are plots of data from string pots 11 and 12. SP11 and SP12, which showed very little displacement, show us that the CLT panels are very rigid. As was anticipated prior to testing, the shear deformation in the wood panels themselves is negligible in design calculations.

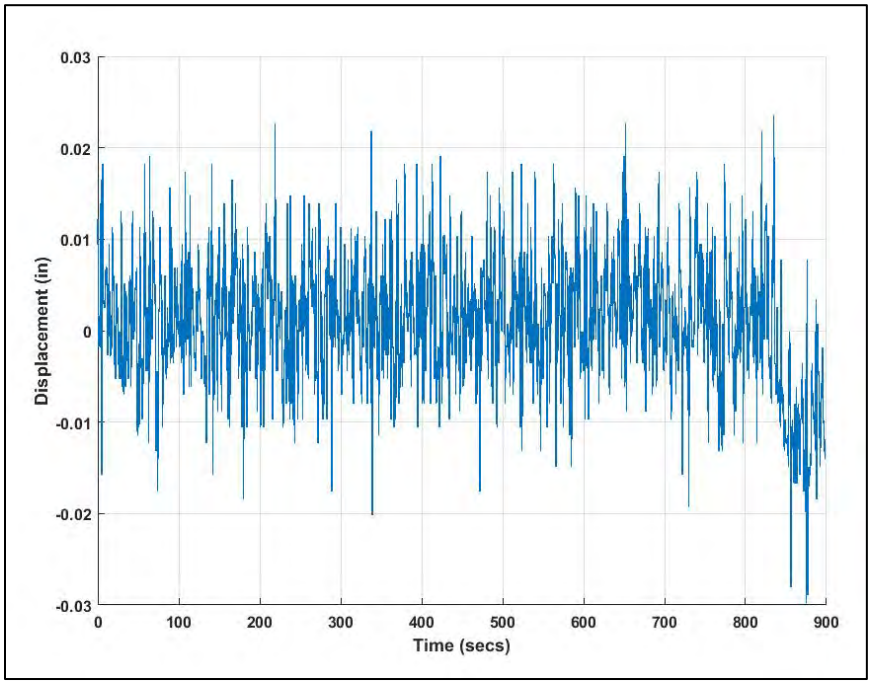

Figure 4.20 String Pot 11 Data

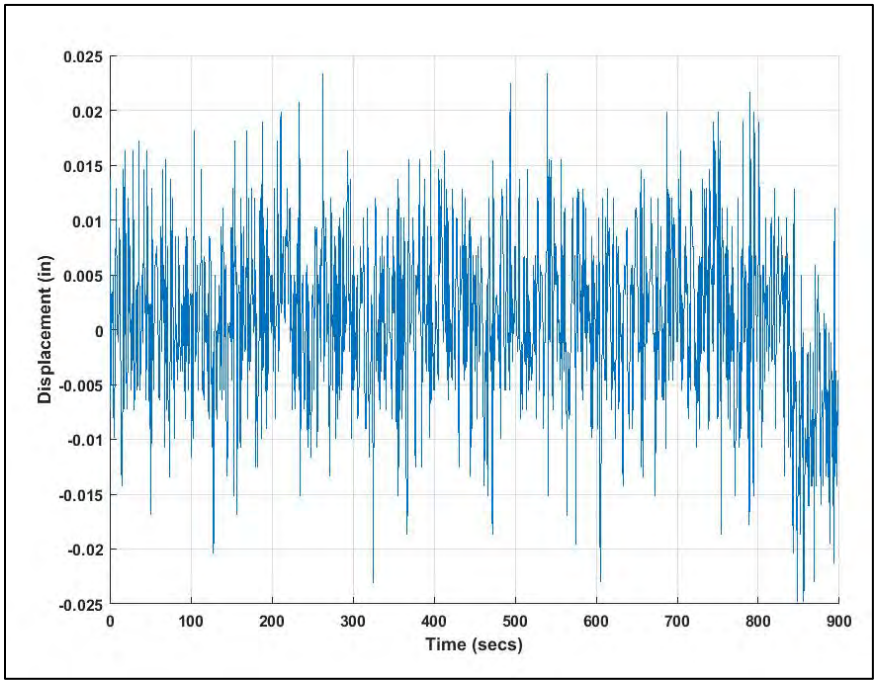

Figure 4.21 String Pot 12 Data

SP13 gives us separation between panels 4 and 5 that are located closest to the fixed end of the cantilever. As can be seen from Figure 4.22, the values were low and there was a gradual increase. The increase in separation was minimal before the SDS screws connecting chord members to the diaphragm failed in shear. After this, the tension load increased on the steel splices. Due to this, the splices started to rotate and nails sheared, resulting in a rapid increase in separation between panels. Then there was a sudden jump in displacement values. This resulted in total failure of the diaphragm.

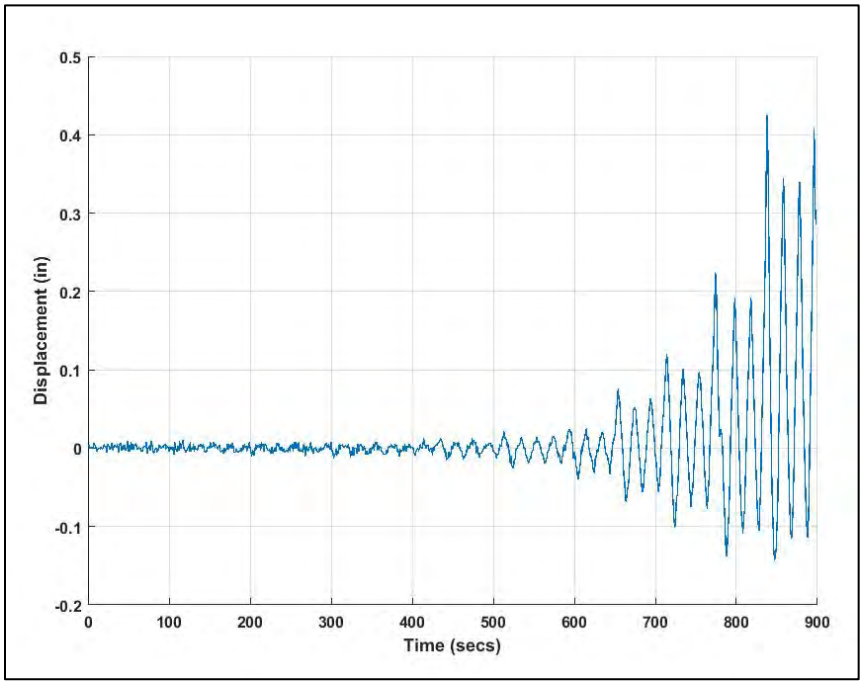

Figure 4.22 String Pot 13 Data

Figure 4.23 is a plot of displacement values of string pots versus distance of string pots from the fixed end of the cantilever. As one can see, the plots are linear for lower displacements. For higher values of actuator displacement, SP4 values are closer to the maximum displacement. As the diaphragm started to fail, the steep increase in values of displacement from SP1 to SP3 to SP4 is very noticeable. This occurred because the chord member connection failed.

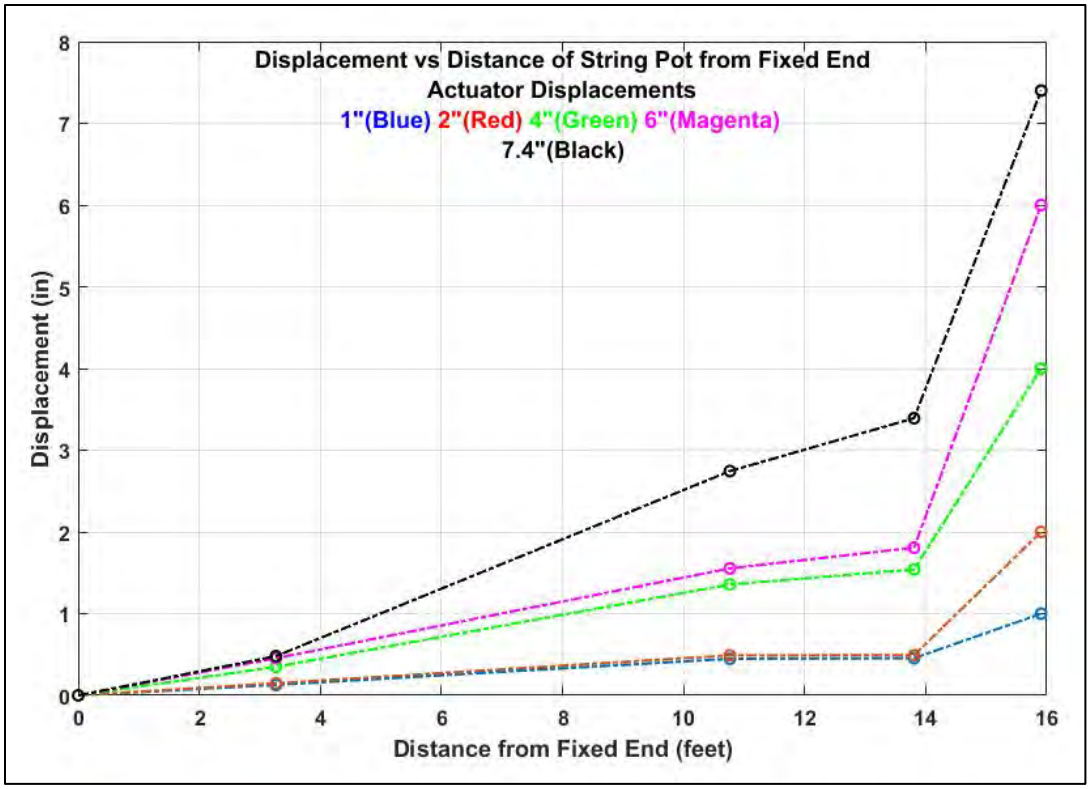

Figure 4.23 Displacement of String Pots vs Distance of String Pots from Fixed End

5. SUMMARY, CONCLUSION AND CONTRIBUTIONS

The CLT diaphragm test presented in this report can serve as a single step in understanding the behavior of CLT diaphragms under seismic loading. E1 category CLT panels were used to form the diaphragm, which was approximately 16.4 ft. by 14 ft. Rough sawn lumber was used for chord members to ensure controlled design strength for testing. The diaphragm was set up as a cantilever beam according to ASTM E455 – 11 specifications. This required that an actuator apply the load on the free end of the diaphragm. The CUREE testing protocol was used with a reference displacement of 3 inches for the final and most meaningful test. From the data and test results, we can see the diaphragm did not behave in the predicted manner. The diaphragm was anticipated to fail in shear, but shear failure of the SDS screws connecting the CLT panels to chord members occurred first. This resulted in an increased tension load acting on the steel splices. Due to this, the steel splice connectors failed in tension. The nails failed in shear and the connectors became dislodged. This led to separation of CLT panels in the north-south direction, which resulted in total failure of the diaphragm.

The drawback of this CLT diaphragm test is the number of tests. Because only one major test was conducted, the data collected do not allow for parametric study. More CLT diaphragm tests of this kind would allow researchers to gather more data. In addition, using a variety of connections in the CLT diaphragm would also allow us to compare connection capacities and their influence on the global behavior of the diaphragm. If different types of CLT are used in conjunction with different types of connections, a meaningful database can be developed. All these data can be used to improve the CLT building and bridge designs.

REFERENCES

Amini, M.O., van de Lindt, J.W., Rammer, D., Pei, S., Line, P., & Popovski, M. (2016). "Determination of Seismic Performance Factors for CLT Shear Wall Systems." *Journal of Earthquake Engineering (2017): 1-21.*

ANSI/APA PRG 320 – 2012 Standard for Performance-Rated Cross-Laminated Timber, APA The Engineered Wood Association, 2012. Tacoma, WA.

ANSI/AWC NDS-2015 National Design Specification (NDS) for Wood Construction, American Wood Council, 2015. Leesburg, VA.

ANSI/AWC NDS-2015 National Design Specification (NDS) Supplement: Design Values for Wood Construction, American Wood Council, 2015. Leesburg, VA.

ANSI/AWC SDPWS-2015 Special Design Provisions for Wind and Seismic, American Wood Council, 2014. Leesburg, VA.

ASCE/SEI 7-10 Minimum Design Loads for Buildings and Other Structures.

ASTM E455-11 Standard Method for Static Load Testing of Framed Floor or Roof Diaphragm Constructions for Buildings, ASTM International, West Conshohocken, PA, 2011, http://www.astm.org/cgi-bin/resolver.cgi?UOP5.

Brandner, R., Dietsch, P., Droscher, J., Schulte-Wrede, M., Kreuzinger, H., Sieder, M., Schickhofer, G., & Winter, S. (2015). "Shear Properties of Cross Laminated Timber (CLT) under in-plane load: Test Configuration and Experimental Study." *INTER Proceedings Meeting 48 2015 (pp. 181-201).*

Breneman, S. (2016). "Cross-Laminated Timber Structural Floor and Roof Design." *Structural Design Magazine, Design Issue for Structural Engineers, June 2016.*

CLT Handbook U.S Edition. (2013). FPInnovations, 2013.

Cobeen, K.E., Dolan, J.D., Thompson, D., & van de Lindt, J.W. (2014). "Seismic Design of Wood Light-Frame Structural Diaphragm Systems: A Guide for Practicing Engineers." *NEHRP Seismic Design Technical Brief No. 10, NIST GCR 14-917-32, ATC, 2014, p.42.*

Earthquake Engineering Research Institute. (EERI). (January 2003). Securing Society Against Catastrophic Earthquake Losses.

Espinoza, O., Trujillo, V.R., Mallo, M.F.L., & Buehlmann, U. (2016). "Cross-Laminated Timber: Status and Research Needs in Europe." *BioRes.* 11(1), 281-295.

Federal Emergency Management Agency (FEMA) P695. (2009). Quantification of Building Seismic Performance Factors.

Fink, G., Frangi, A., & Kohler, J. (2015). "Bending tests on GLT beams having well-known local material properties." *Materials Structures, 48, 3571-3584 (2015).*

ICC ESR – 2236. (2017) Simpson Strong-Tie Company Inc., 5956 West Las Positas Boulevard, Pleasanton, California, 94588.

Krawinkler, H., Parisi, F., Ibarra, L., Ayoub, A., & Medina, R. (2001). “Development of a Testing Protocol for Woodframe Structures.” Richmond, CA. *Earthquake Engineering & Structural Dynamics 34.12 (2005): 1489-1511.*

Pei, S., van de Lindt, J.W., Popovski, M., Berman, J.W., Dolan, J.D., Ricles, J., Sause, R., Blomgren, H., & Rammer, D.R. (2016). “Cross-Laminated Timber for Seismic Regions: Progress and Challenges for Research and Implementation.” *Journal of Structural Engineering 142, no. 12 (2016): 02516001.*

Schickhofer, G., Brandner, R., & Bauer, H. (2016). Product Properties and Strength Classes of CLT.

Spickler, K., Closen, M., Line, P., & Pohll, M. (2015) “Cross Laminated Timber Horizontal Diaphragm Design, Rv10-12, October 2015.” *CLT White paper*.

APPENDICES

APPENDIX A. CLT DIAPHRAGM TEST SETUP

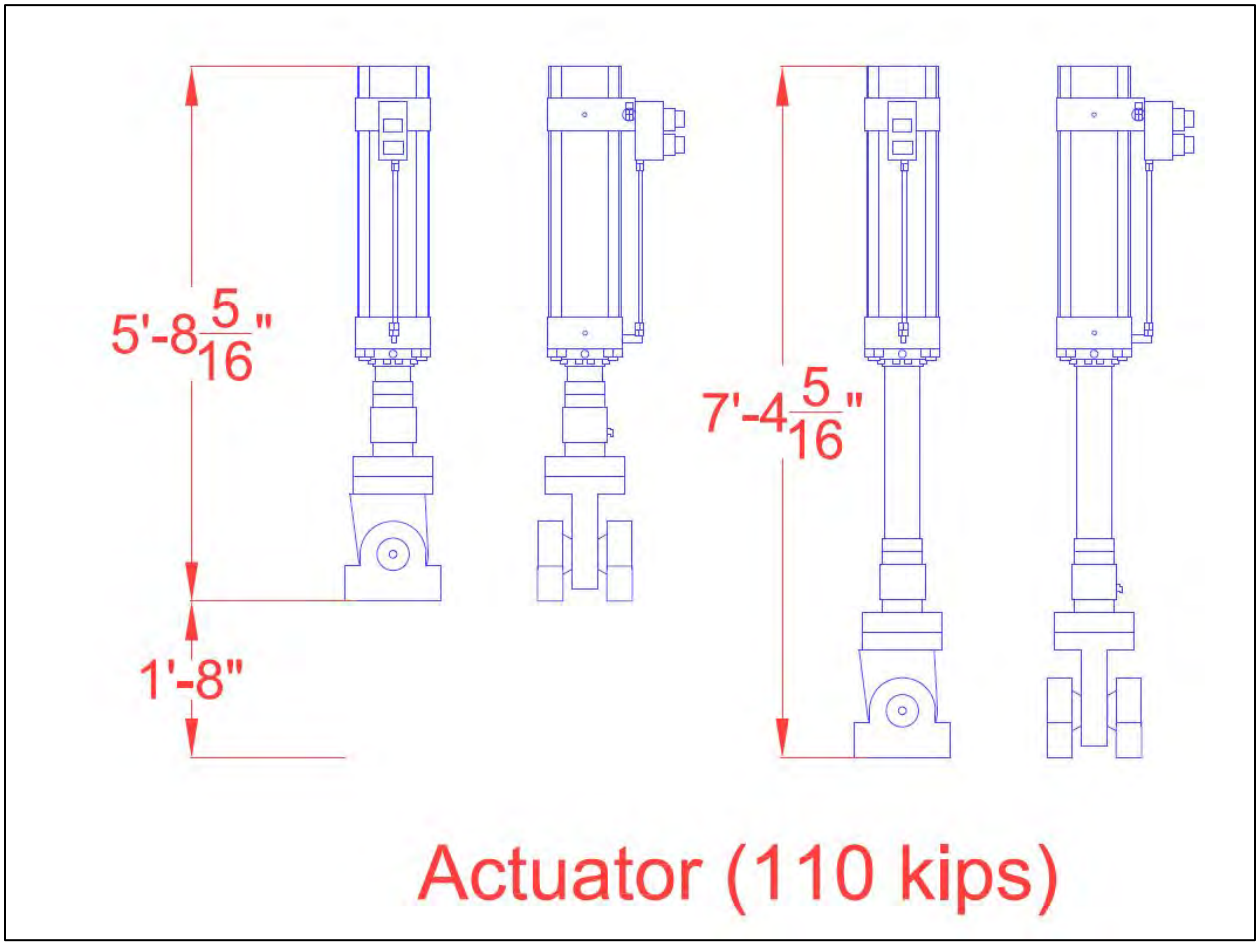

Figure A.1 Actuator Top and Side Views (Fully Compressed and Fully Elongated)

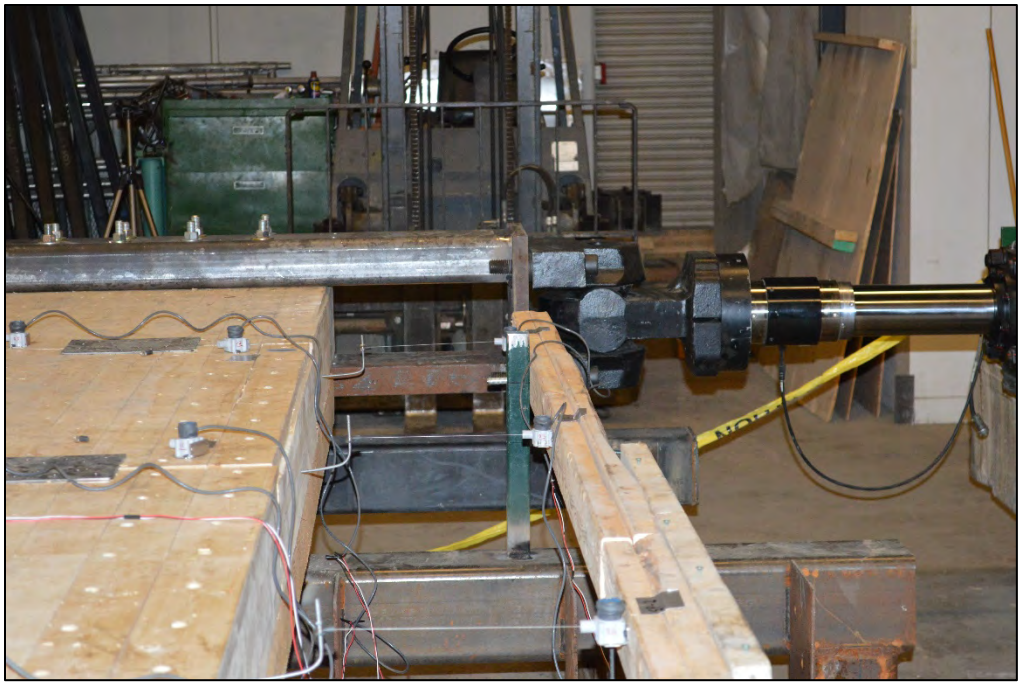

Figure A.2 Test Setup View

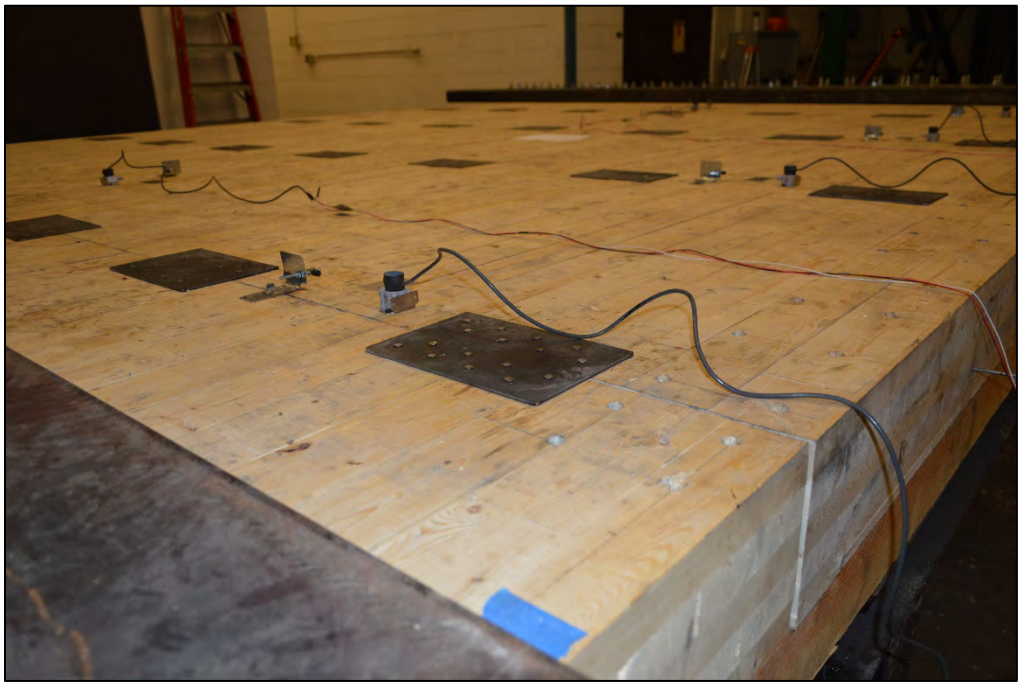

Figure A.3 Test Setup View

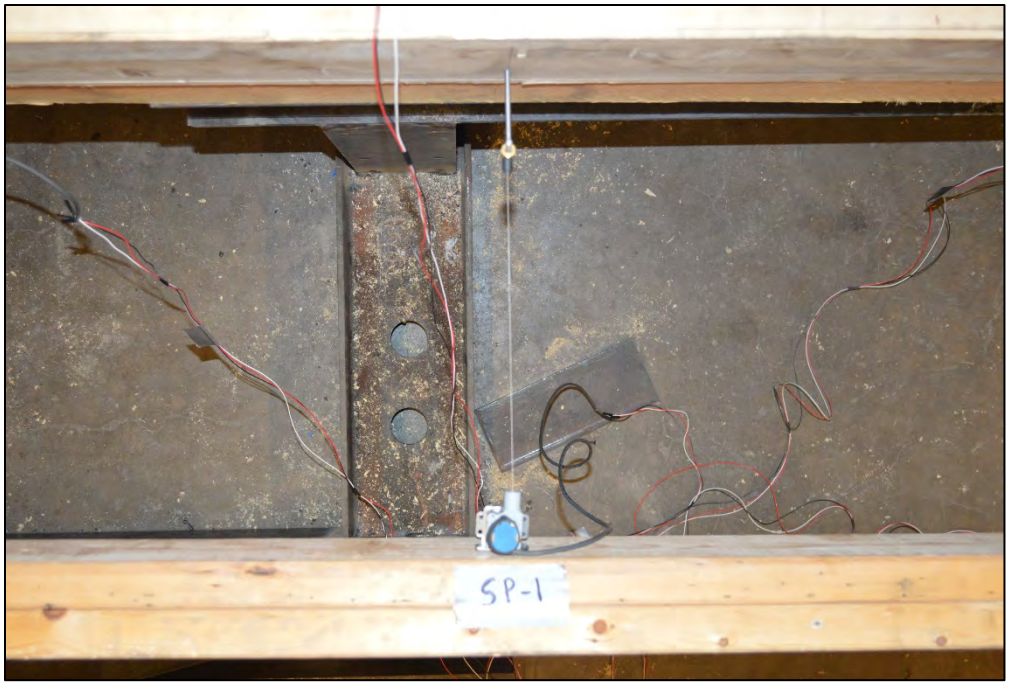

Figure A.4 SP1 Top View

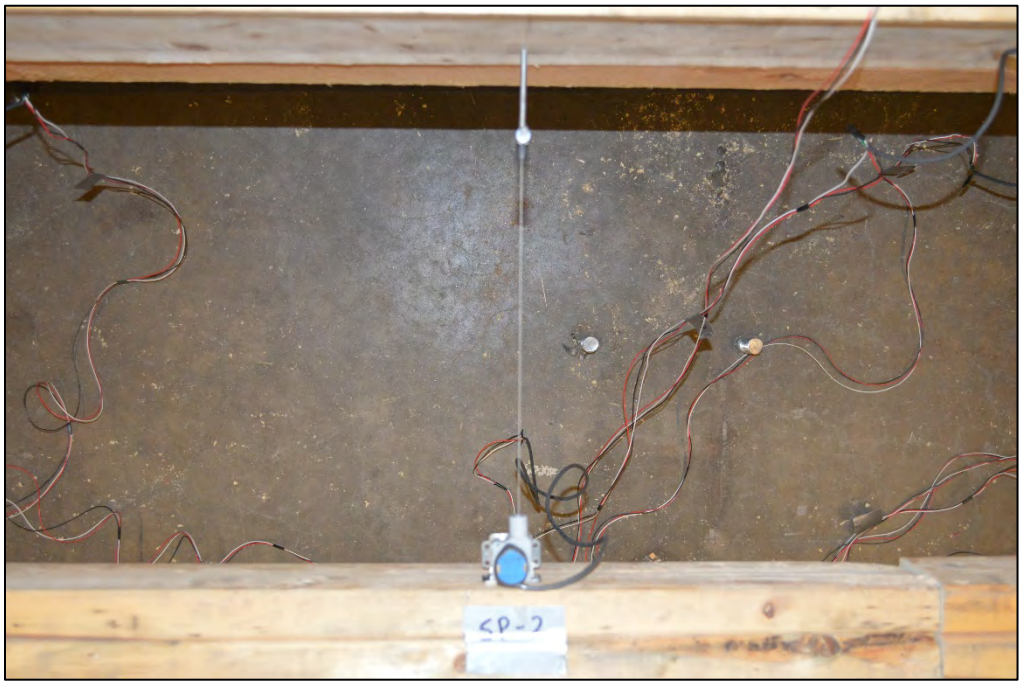

Figure A.5 SP2 Top View

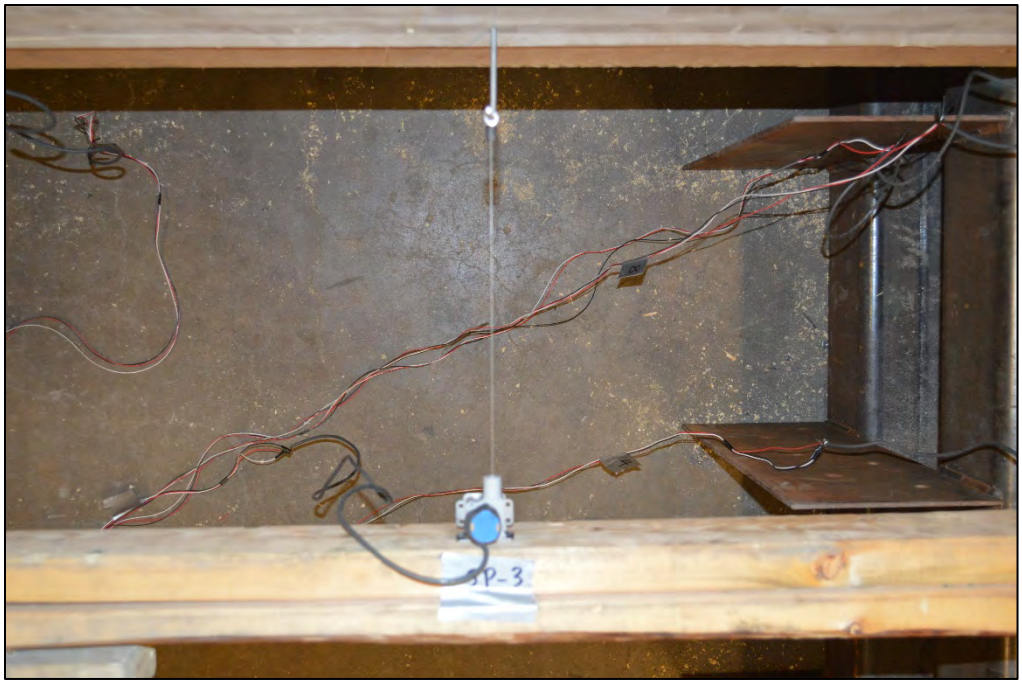

Figure A.6 SP3 Top View

Figure A.7 SP4 Top View

Figure A.8 SP5 Top View

Figure A.9 SP6 Top View

Figure A.10 SP7 Top View

Figure A.11 SP8 Top View

Figure A.12 SP9 Top View

Figure A.13 SP10 Top View

Figure A.14 SP11 Top View

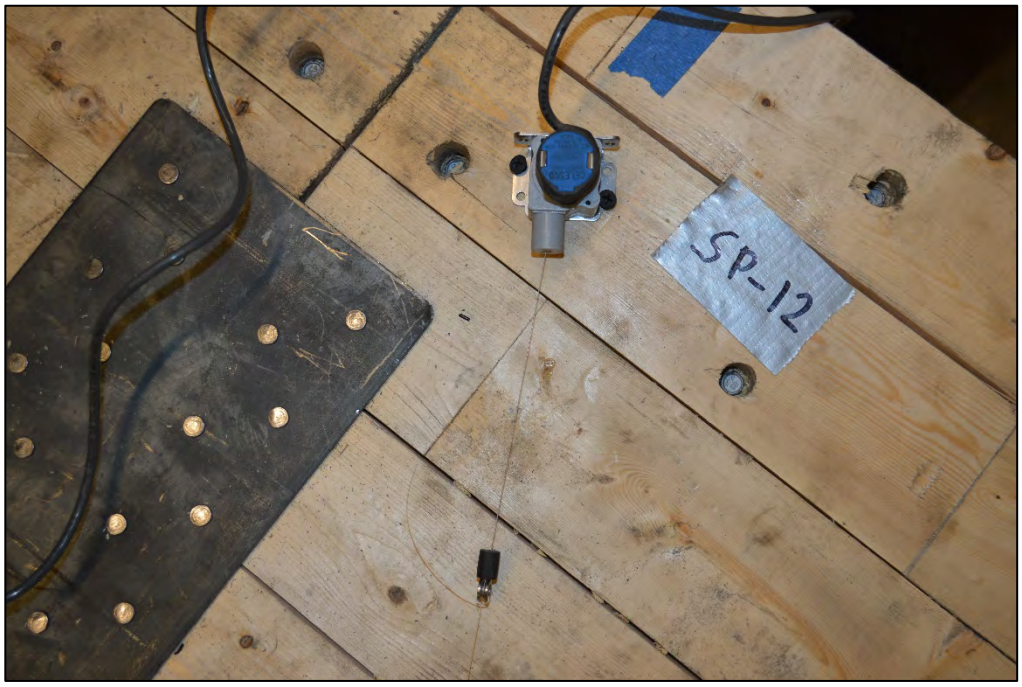

Figure A.15 SP12 Top View

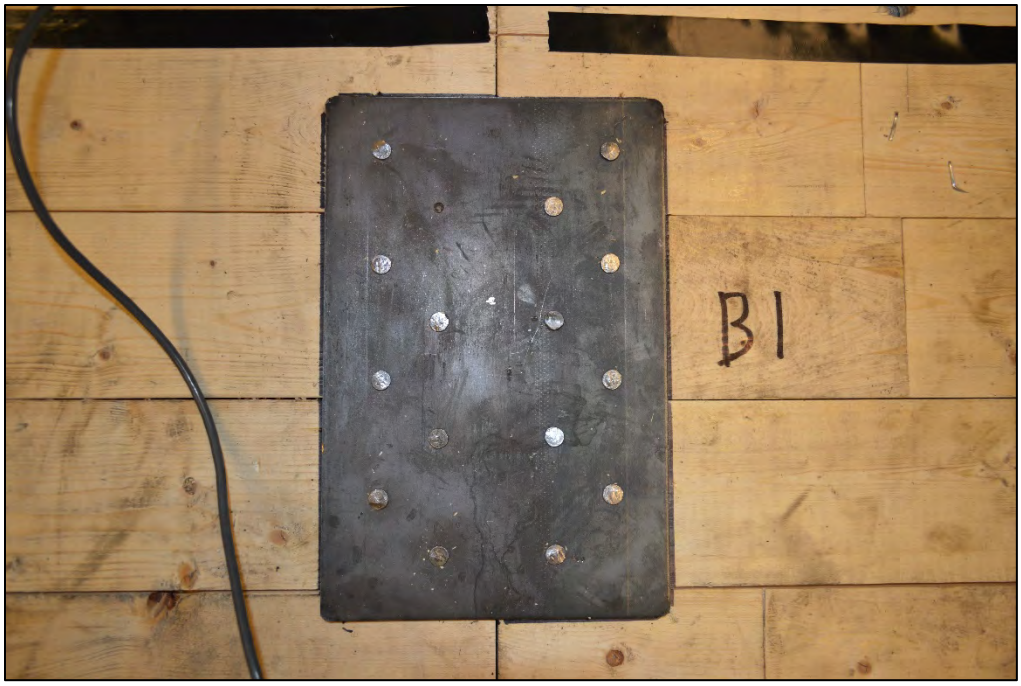

Figure A.16 Connector B1 before the Test

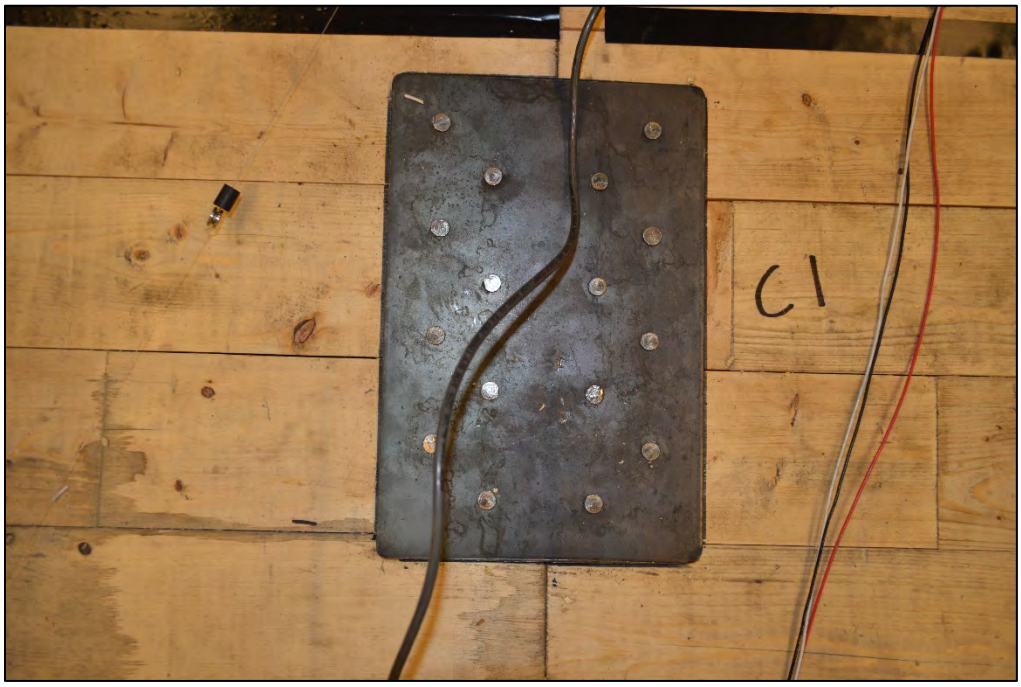

Figure A.17 Connector C1

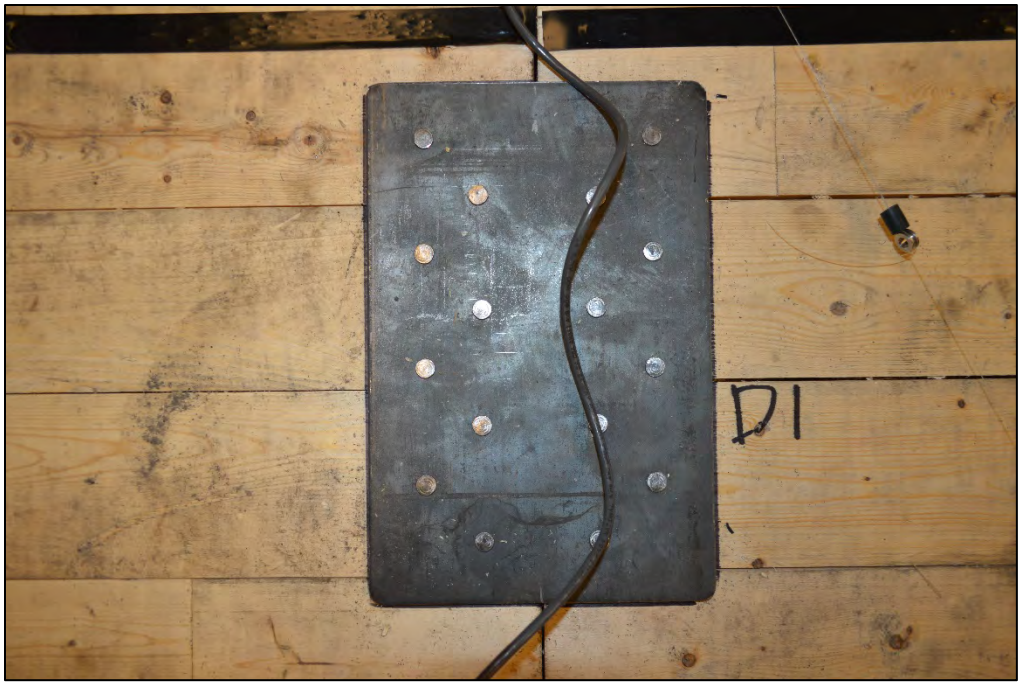

Figure A.18 Connector D1

Figure A.19 HDU Hold-down

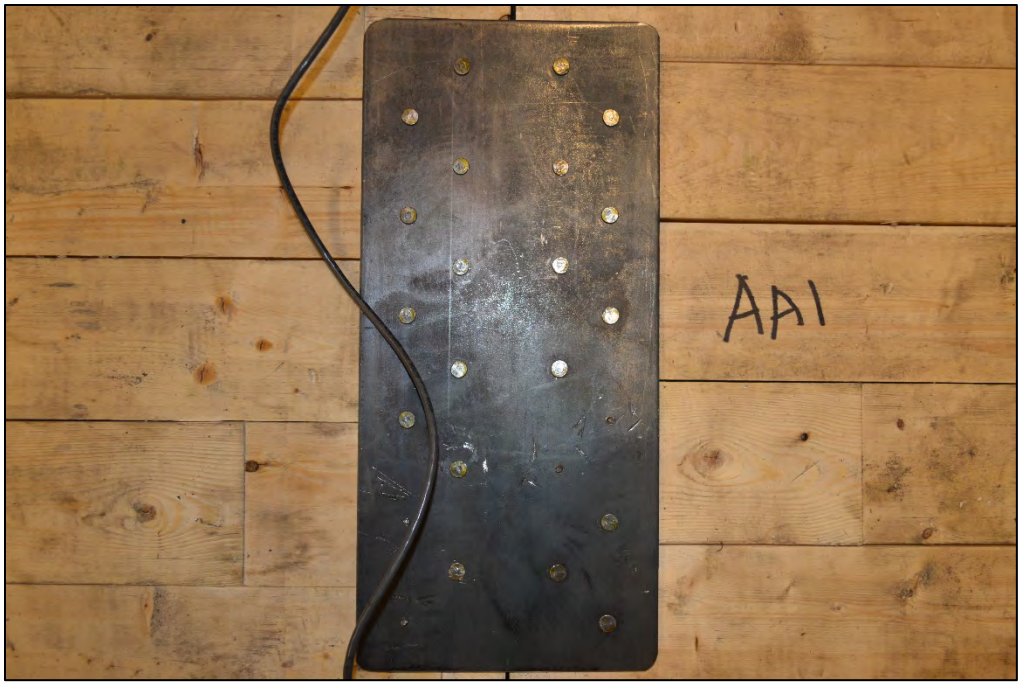

Figure A.20 Connector AA1

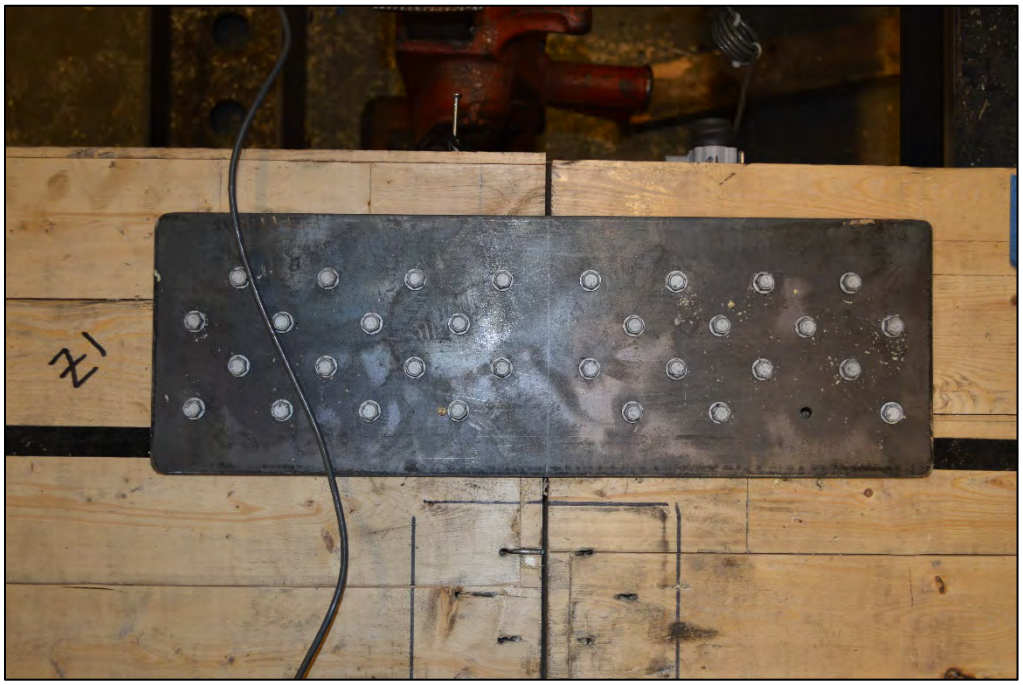

Figure A.21 Connector Z1

Figure A.22 West End of the Test Setup

Table A.1
SDS Wood Screw Specifications, Bending Yield Strength, And Fastener Allowable Steel Strength (ICC ESR-2236)

FASTENER DESIGNATION (based on point geometry)			HEAD MARKING	SCREW SPECIFICATIONS (inches)				SPECIFIED BENDING YIELD STRENGTH[3], F_{yb} (psi)	FASTENER ALLOWABLE STEEL STRENGTH[4] (lbf)	
Carbon Steel		Stainless Steel		Screw Length, *L1*	Thread Length[1], *T*	Unthreaded Shank Length, *L1* ! *T*	Minor Thread (root) Diameter[2], *D*,		Tension	Shear
Type 17 Point	Four-Cut Point	Type 17 or Four-Cut Point								
SDS 1/4x1 1/2	SDS25112	SDS25112SS	S1.5	1 1/2	1	1/2	0.185	164,000	1,430	800
SDS 1/4x1 3/4	SDS25134	—	S1.75	1 3/4	1 1/4	1/2				
SDS 1/4x2	SDS25200	SDS25200SS	S2	2	1 1/4	3/4				
SDS 1/4x2 1/2	SDS25212	SDS25212SS	S2.5	2 1/2	1 1/2	1				
SDS 1/4x3	SDS25300	SDS25300SS	S3	3	2	1				
SDS 1/4x3 1/2	SDS25312	SDS25312SS	S3.5	3 1/2	2 1/4	1 1/4				
SDS 1/4x4 1/2	SDS25412	—	S4.5	4 1/2	2 3/4	1 3/4				
SDS 1/4x5	SDS25500	—	S5	5	2 3/4	2 1/4				
SDS 1/4x6	SDS25600	—	S6	6	3 1/4	2 3/4				
SDS 1/4x8	SDS25800	—	S8	8	3 1/4	4 3/4				

For **SI:** 1 inch = 25.4 mm, 1 psi = 6.89 kPa, 1 lbf = 4.45 N.

[1]Length of thread includes tip. See Figure 1.
[2]Minor thread diameter shown in the table is the nominal diameter with manufacturing tolerances from a minimum of 0.183 inch to a maximum of 0.193 inch.
[3]Bending yield strength determined in accordance with ASTM F1575 using the minor thread (root) diameter, D_r.
[4]Allowable fastener strengths are based on steel properties of the screw. Refer to Tables 2 and 3 for allowable reference lateral (*Z*) design values for steel-to-wood and wood-to-wood connections, respectively.

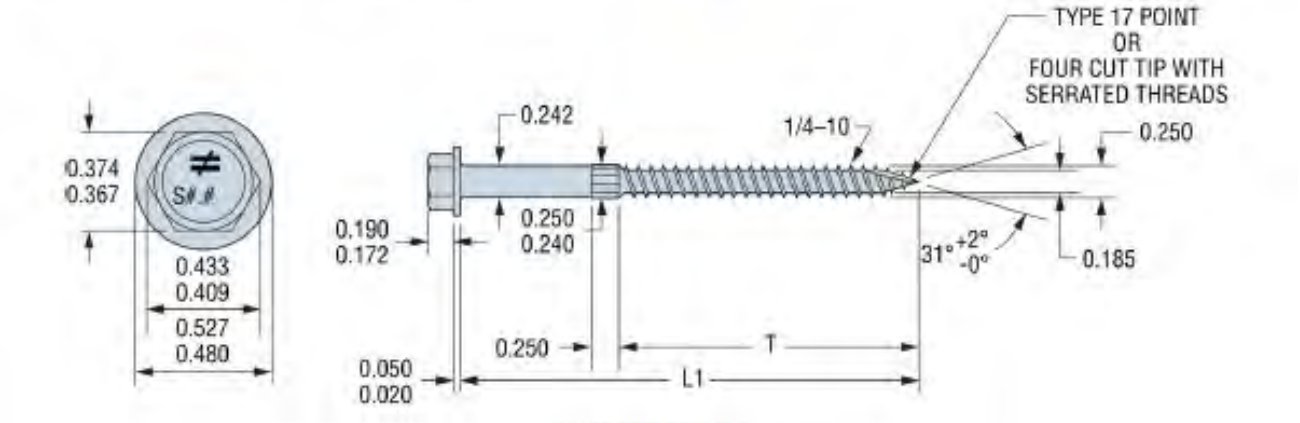

U.S. Patent 6,109,850; 5,897,280; 7,101,133

FIGURE 1—SDS SCREW

Table A.2
Reference Lateral Design Values (Z) for Single Shear Steel-to-Wood Connections with SDS Wood Screws[1,2] (ICC ESR-2236)

SCREW LENGTH (inches)	STEEL SIDE MEMBER DESIGN THICKNESS[3,4], t_s (inches)					
	0.0584 (No. 16 gage)	0.0721 (No. 14 gage)	0.1026 (No. 12 gage)	0.1342 (No. 10 gage)	0.1795 (No. 7 gage)	0.2405 (No. 3 gage)
	Lateral Design Value (Z)[5,6,7] (lbf)					
1½	250	250	250	250	250	250
1¾	250	250	250	250	250	250
2	250	290	290	290	290	290
2½	250	390	390	420	420	420
3	250	420	420	420	420	420
3½	250	420	420	420	420	420
4½	250	420	420	420	420	420
5	250	420	420	420	420	420
6	250	420	420	420	420	420
8	250	420	420	420	420	420

For SI: 1 inch = 25.4 mm, 1 lbf = 4.45 N, 1 ksi = 6.89 MPa.

[1]The side member must be steel having a minimum tensile strength (F_u) equal to 45 ksi when the steel member design thickness is from 0.0584 inch to 0.1795 inch, and a minimum F_u equal to 52 ksi when the steel member design thickness is 0.2405 inch.
[2]The main member must be wood having a minimum assigned specific gravity of 0.50, such as Douglas fir–larch, and must be sufficiently sized to accommodate the screw length less the thickness of the side member. Values are also applicable for fasteners installed into the face of engineered wood described in Section 3.2.2.
[3]The uncoated minimum steel thickness of the cold-formed product delivered to the jobsite must not be less than 95 percent of the tabulated design thickness, t_s.
[4]Holes in the steel side member must be predrilled or prepunched. Hole diameter must comply with Section 3.2.3 of this report.
[5]Tabulated lateral design values (Z) must be multiplied by all applicable adjustment factors, including the load duration factor, C_D, from the NDS as referenced in the IBC or IRC.
[6]Screws must be installed into the side grain of the wood main member with the screw axis perpendicular to wood fibers.
[7]Minimum fastener penetration must be equal to the screw length less the thickness of the metal side plate.

APPENDIX B. CLT DIAPHRAGM TEST RESULTS

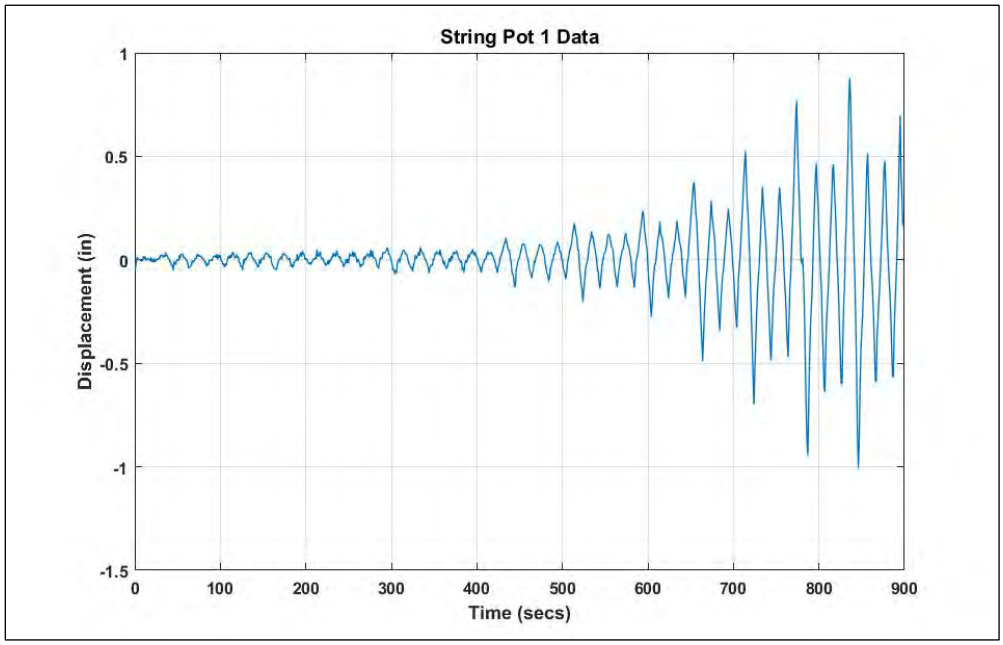

Figure B.1 SP1 Data

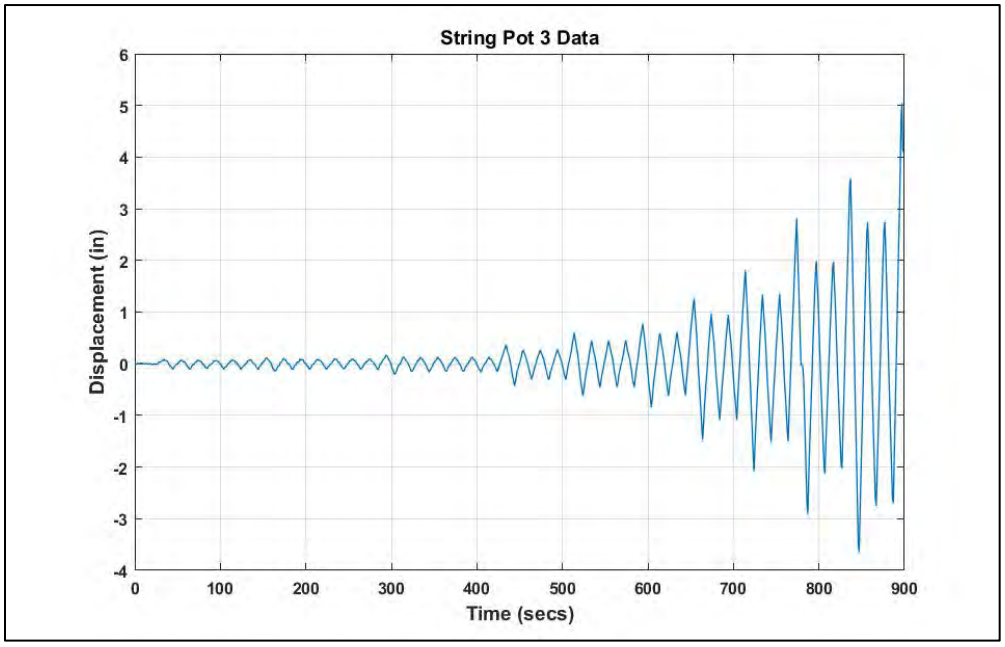

Figure B.2 SP3 Data

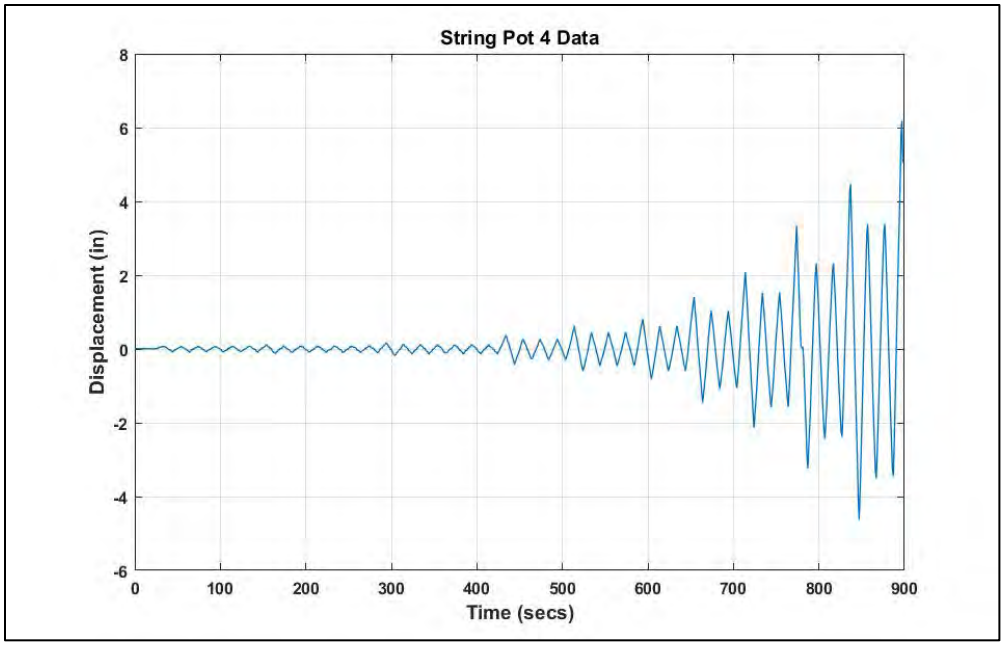

Figure B.3 SP4 Data

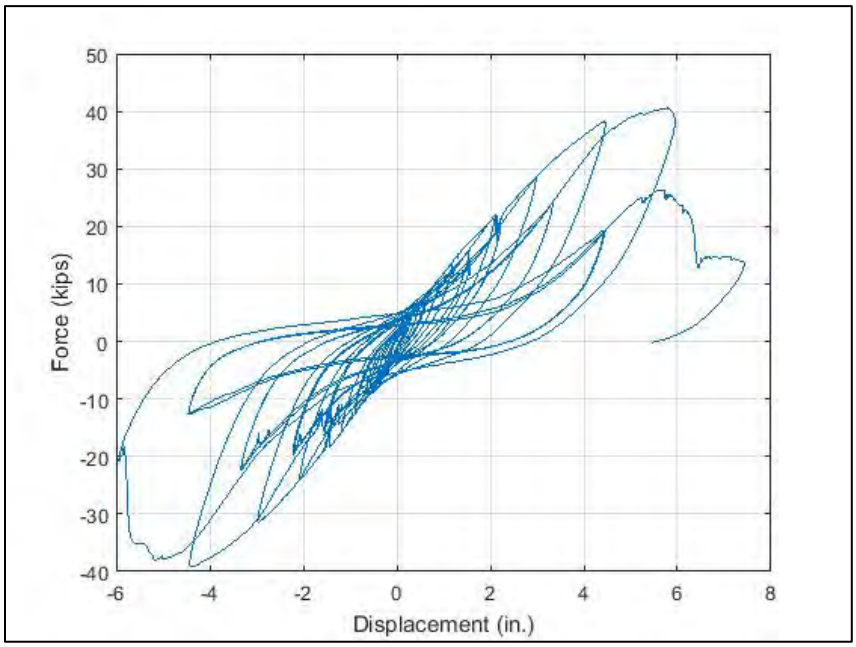

Figure B.4 Hysteresis Plot